Forschungszentrum Karlsruhe
in der Helmholtz-Gemeinschaft

Wissenschaftliche Berichte
FZKA 6883
SAM-COLOSS-P027

TG-Rig Tests (Thermal Balance) on the Oxidation of B_4C

Basic Experiments, Modelling and Evaluation Approach

W. Krauss, G. Schanz, H. Steiner

Institut für Materialforschung
Programm Nukleare Sicherheitsforschung

Oktober 2003

Forschungszentrum Karlsruhe

in der Helmholtz-Gemeinschaft

Wissenschaftliche Berichte

FZKA 6883

SAM-COLOSS-P027

TG-Rig Tests (Thermal Balance) on the Oxidation of B_4C

Basic Experiments, Modelling and Evaluation Approach

W. Krauss, G. Schanz, H. Steiner

Institut für Materialforschung

Programm Nukleare Sicherheitsforschung

Forschungszentrum Karlsruhe GmbH, Karlsruhe

2003

Impressum der Print-Ausgabe:

Als Manuskript gedruckt

Forschungszentrum Karlsruhe GmbH
Postfach 3640, 76021 Karlsruhe

Mitglied der Hermann von Helmholtz-Gemeinschaft
Deutscher Forschungszentren (HGF)

ISSN 0947-8620

Abstract

In the frame of a separate-effects test program extensive studies on the oxidation of boron carbide using a Thermal Balance Testing System (**T**hermo-**G**ravimetry TG) were performed. The test series included besides the oxidation tests on B_4C, also examinations on B_4C oxidation related compounds (e.g. B_2O_3). The evaluation and interpretation of the experiments was supported by basic modelling with respect to the understanding of occurring mechanisms and first determination of reaction kinetics parameters.

The oxidation tests on B_4C pellets were performed in the temperature range 600 to 1300 °C under flowing Ar/O_2 and wet Ar atmosphere. Two types of pellets were investigated, the first ones had high density (TD = 98%) and the second ones were porous reactor typical absorber pellets (Framatome, TD = 72%).

The evaporation tests on B_2O_3 were conducted in dry flowing Ar and wet Ar atmosphere, in the same temperature range as the B_4C oxidation tests. Wet Ar was produced by passing the Ar stream through a heated water bath with an adjustable temperature between 20 and 60 °C.

The performed tests showed that evaporation of B_2O_3 and oxidation of B_4C is strongly depended on environment conditions. Several mechanisms with different reaction kinetics and dependencies e.g. on temperature are interacting. In simplification the oxidation of B_4C is governed by the formation of B_2O_3 and by the transportation of the boron oxide in the gas phase. This results for long test times under wet Ar atmosphere and other stationary conditions in a constant consumption of B_4C. Porous samples show a more complex and accelerated reaction behaviour compared to dense pellets. At least for modelling of the short time behaviour porosity effects have to be included.

Using the developed modelling tools it could be shown that TG tests and BOX-rig tests, measuring different parameters (mass change and H_2 production, respectively) and working under different environmental conditions, can be compared and lead to the same general oxidation behaviour.

Untersuchungen zur Oxidation von B_4C mittels Thermowaage - Tests

Grundlegende Experimente, Modellierung und Auswertungsansätze

Abstract

Im Rahmen eines Einzeleffekt-Testprogrammes wurden weit reichende Untersuchungen zur Oxidation von Borkarbid in einem Thermowaagesystem ausgeführt. Die Testserien zur Oxidation von B_4C umfassten auch die Untersuchung von Verbindungen wie z.B. B_2O_3, die bei der Reaktion von B_4C in oxidierender Atmosphäre gebildet werden. Die Auswertung und Interpretation der Experimente wurde durch grundlegende Modellierungsarbeiten unterstützt. Diese sollten zum klareren Verständnis der auftretenden Reaktionsmechanismen beitragen und zusätzlich dazu eine erste Auswertung der Reaktionskinetik erlauben.

Die Versuche zur Oxidation von B_4C wurden im Temperaturbereich 600 bis 1300 °C in strömendem Ar/O_2 Gemisch der Zusammensetzung 80/20 Vol.% und in feuchter Ar Atmosphäre ausgeführt. Eingesetzt wurde 2 Arten von B_4C Pellets. Erstere Art hatte eine Dichte von ca. 98 %. Die zweite Sorte war reaktortypisches poröses Absorbermaterial mit einer Dichte von ca. 72 % (Framatome).

Untersuchungen zur Verdampfung von B_2O_3 erfolgten in fließender trockener und feuchter Ar-Atmosphäre bei gleichen Temperaturbedingungen wie die Oxidationstests. Der feuchte Ar-Strom wurde mittels Durchleiten von trockenem Ar durch ein temperaturgeregeltes Wasserbad im Bereich von 20 bis 60 °C erzeugt.

Die durchgeführten Tests zeigten, dass die Verdampfung von B_2O_3 und die Oxidation von B_4C stark von den Umgebungsbedingungen abhängen. Mehrere Reaktionsmechanismen mit unterschiedlicher Reaktionskinetik und verschiedenen Abhängigkeiten von Versuchsparametern (z.B. Temperatur) treten parallel zueinander auf und stehen gegenseitig miteinander in Wechselwirkung. Die Oxidation von B_4C wird in erster Näherung durch die Bildung von B_2O_3 und durch den Transport von Boroxid in der Gasphase bestimmt. Im Bereich von Langzeittests führt dies zu einem konstanten Verbrauch von B_4C bei der Oxidation in feuchtem Ar-Strom und sonst unveränderten Versuchsbedingungen. Im Gegensatz zu dichten Proben zeigen poröse Pellets ein komplexeres Reaktionsverhalten und höhere Reaktionsraten. Mindestens zur Erzielung einer zutreffenden Beschreibung des Kurzzeitverhaltens müssen Poreneffekte mitberücksichtig und in die Modellierung integriert werden.

Durch Anwendung der entwickelten Modelle konnte gezeigt werden, dass die beiden Versuchsstände – Thermowaagesystem und Box-Teststand – gleiches Reaktionsverhalten für die Oxidation von B_4C liefern, obwohl unterschiedliche Prozessparameter erfasst werden (Masseänderung bzw. H_2-Produktion) und unterschiedliche Umgebungsbedingungen vorliegen.

Contents

1. Introduction

The Thermo-gravimetric examinations on the oxidation behaviour of B_4C are part of the COLOSS (Core Loss during a Severe Accident) project. Under this project the effects of B_4C, an absorber material used in reactors of type BWR, PWR and VVER, on different objectives like H_2 source term, melt generation or CH_4 production during a severe accident are examined [1, 2]. The aim of the TG-tests is to deliver fundamental B_4C oxidation data, mostly directed on identification of reaction phenomena and mechanisms and determination of reaction kinetics.

In contrast to the oxidation of cladding materials e.g. Zry-4, where only non volatile oxides are formed, the oxidation products of B_4C are more or less volatile. Direct evaluation of mass change data as produced by Thermo-Gravimetry require, due to this material behaviour, additional information like evaporation rates of B_2O_3 in dependence of temperature and environmental conditions or test conducts where evaporation is negligible.

By these reasons the experimental part of this separate effects test program performed at Research Centre Karlsruhe was divided into three main parts:

Determination of evaporation behaviour of B_2O_3
Testing of oxidation behaviour of B_4C
Development of first modelling tools for evaluation of B_4C tests

The TG-tests were executed in flowing atmospheres of Ar, Ar/O_2 and steam saturated Ar and test temperatures ranged between 600 and 1300 °C. Gas quality of Ar and O_2 was 5N and 4N, respectively, without additional cleaning or drying measures. In contrast to the BOX-tests [3, 4], which were also part of the separate effect test program at FZK and apply a reaction gas analysing method to determine the oxidation behaviour, the TG-tests use a simultaneous measurement of sample temperature and mass change as function of test to provide the relevant data.

2. Experimental TG set-up

The used thermo-analysing system consists of a combined DTA and TG unit with vertical orientation of the test section, a gas supply system and PC data collection. In Fig. 1 a sketch drawing of the Thermo-balance system is given. In contrast to simple furnaces TG-systems require protection of the sensitive balance system against contamination by reaction products and steam. Caused by this reason the balance housing has to be run through by a protection or purge gas stream and the reaction gas has to be introduced into the reaction zone. These measures result in a more complex gas mixing than known from furnace tests and also in some limitations of test parameters. So formerly planned test temperatures of about 1450 °C, which were earlier used in Zry-4 tests without problems, had to be reduced to the level of 1300 °C, and the ratio of reaction gas to purge gas had not to overshoot 2 to avoid transport of reaction products, mainly boric acids, into the balance housing.

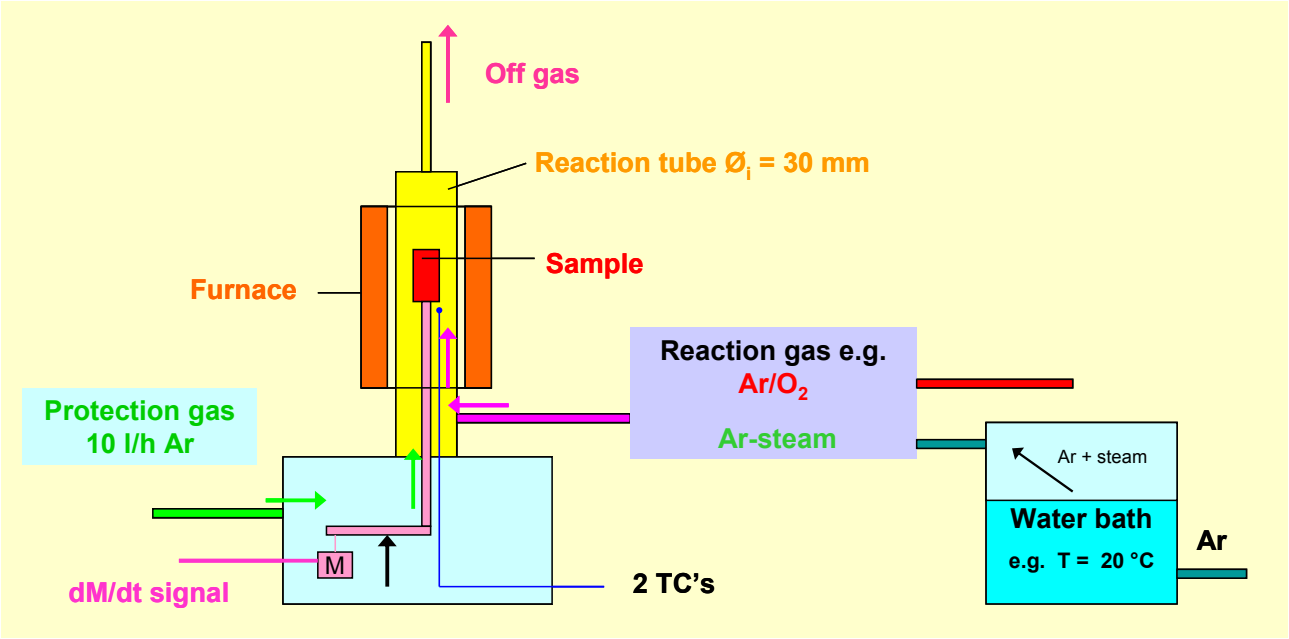

Fig. 1: Schematic drawing of the used Thermal-Balance System

3. Materials for TG tests:

Besides some specific scoping tests with graphite and B_4C powders the TG experiments on evaporation and oxidation behaviour were performed on B_2O_3 powders and B_4C pellets. The specifications of the test materials and other typical data are given in Tab. 1.

Material	Shape Supplier	Typical dimension [mm]	Typical weight [mg]	Density % TD	Atmosphere
C	Pellet SGL	Ø 6.0 x 10.0	360	98	Ar / O_2 20% Ar / steam 20 °C
B_2O_3	Powder ROTH	2 µm UHV-dried	800	-	Ar Ar / steam 20 °C Ar / steam 60 °C
B_4C	Powder HITEC	Approx. 20 µm	300	Appr. 55	Ar / O_2 20%
B_4C	Pellet Framatome	Ø 14.01 x 7.47 +/- .05	1107	71	Ar / O_2 20% Ar / steam 20 °C Ar / steam 60 °C
B_4C	Pellet ESK	Ø 14.00 x 10.545 +/- .05	3064	98	Ar / O_2 20% Ar / steam 20 °C Ar / steam 60 °C

Tab. 1: Used test materials for TG experiments

Annealing and TG tests were carried out under inert conditions on B_4C and B_2O_3 to determine volatile contaminations and to define conditions for pre test treatments to have defined starting conditions, because it is well known that B_2O_3 absorbs H_2O easily. Also some scoping tests were performed with pure graphite in dry Ar/O_2 and 'wet' Ar atmosphere.

4. TG tests

4.1 Oxidation of graphite:

Some scoping tests were performed with ultra pure C-pellets (Ø = 5 mm, h = 10 mm) to see the response of the TG-system on oxidation of a material which will not form passivating scales. Tests were performed in dry Ar-O_2 and wet Ar atmosphere. Ar gas was saturated by steam at 25 °C. Beginning of an oxidation attack in Ar-O_2 atmosphere was found to take place at around 500 °C. A significant oxidation reaction was detected at 600 °C with a rate of 2.6 mg/h. The reaction rate increases with temperature. At 1000 °C a carbon consumption of 850 mg/h was detected. Under fixed reaction conditions consumption of C over time is constant.

Reaction of C in Ar-steam mixtures reaches also a significant rate at 600 °C, however at a lower level compared to Ar-O_2 atmosphere. At 600 °C the rate was 0.25 mg/h at an offered O_2 amount (from H_2O) of about 200 mg/h and an Ar-steam flow of 10 l/h.

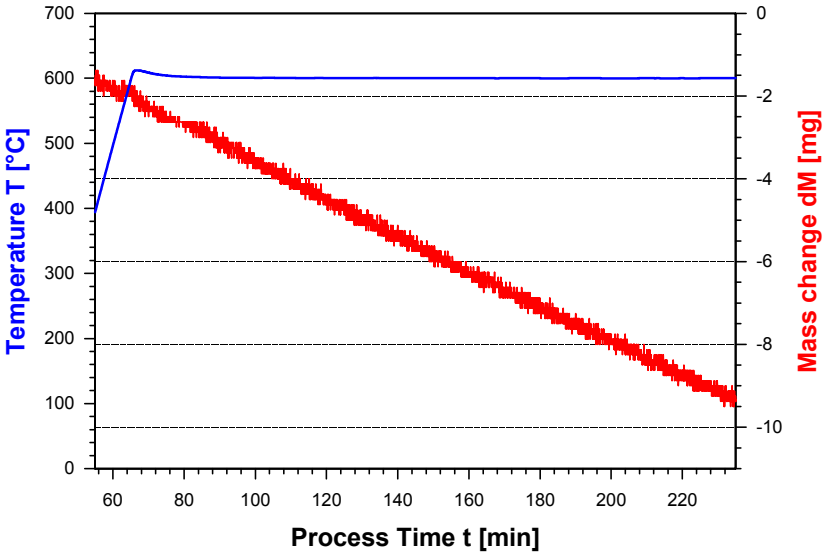

Fig. 2: Oxidation of C-pellet in Ar-O_2, ratio 80/20.
Active surface 2 cm², T = 600 °C
Reacted carbon dM = 2.6 mg/h

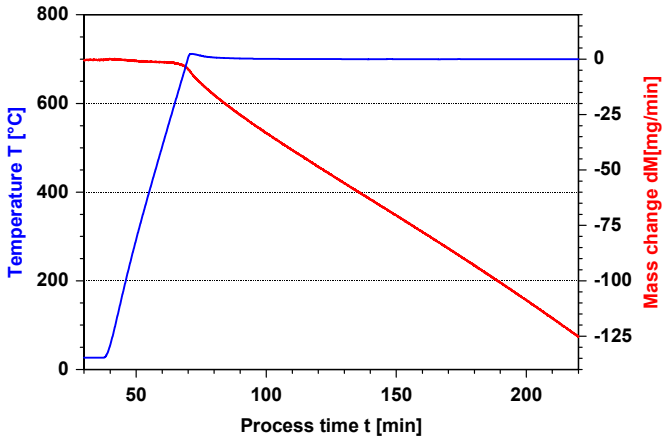

Fig. 3: Oxidation of C-pellet at 700 °C in Ar-O_2 ,
active surface 2 cm², reacted carbon dM = 45 mg/h

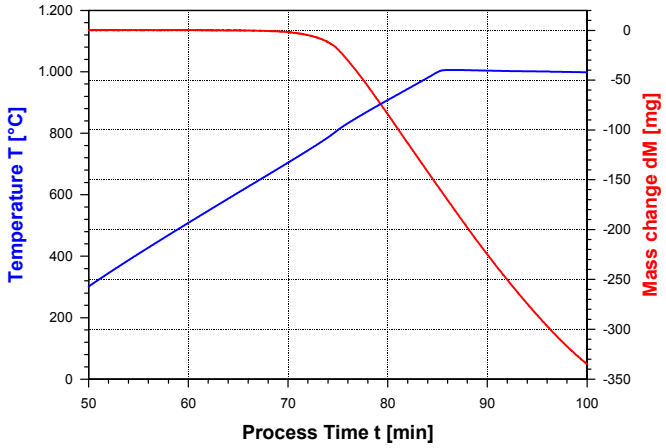

Fig 4: Oxidation of C-pellet at 1000 °C in Ar-O_2
Active surface 2 cm², reacted carbon 850 mg/h

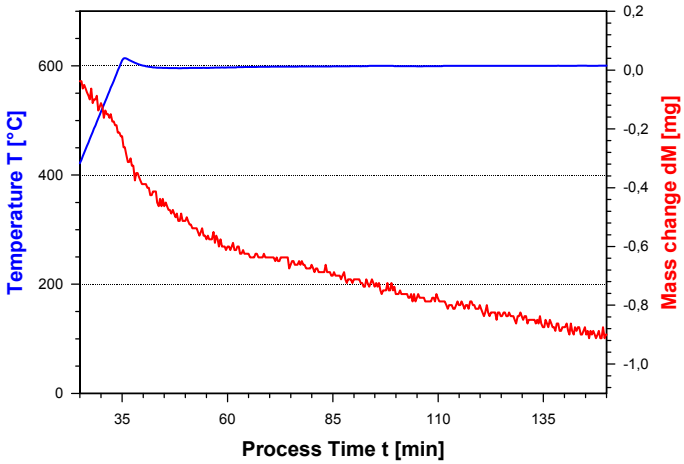

Fig. 5: Oxidation of C-pellet in Ar-steam. active surface 2 cm²,
p(H_2O) = 30 mbar, T = 600 °C
Reacted carbon dM = 0.25 mg/h

4.2 Behaviour of B_2O_3 at low temperatures

For B_2O_3 vacuum annealing at 320 °C was chosen as heat treatment method to prevent melting of the powder. Melting of the hexagonal α-form is expected at 450 °C and softening of the vitreous form between 325 and 450 °C. Density of commercial B_2O_3 is about 1.84 g/cm³, whereas dried B_2O_3 exhibits a lower value of about 1.82 g/cm³. The density of B_2O_3 quenched from about 1000 °C is near 1.50 g/cm² caused by higher degree of molecular disorder. This density is similar to the density of crystalline H_3BO_3 with 1.46 g/cm³, however H_3BO_3 is volatile if humidity is present. It is said that evaporation rates of HBO_2 and B_2O_3 are much smaller caused by coordination effects.

Vacuum drying of commercial B_2O_3 powder at a pressure of $8*10^{-6}$ mbar and 320 °C for 24 h resulted in a mass loss of about 4.25 %. Short time handling of these dried powders under air at RT resulted in a weight gain by absorption of humidity. In Fig. 6 the mass signal of a TG test performed on vacuum dried B_2O_3 powder is given, which was filled into a Y_2O_3 crucible and mounted into the TG-system under air. The mass decrease during the heat up phase indicates, that the powder absorbed humidity during handling. Additionally it can be seen, that no further mass decrease takes place after a certain time at 700 °C (isothermal test phase). This behaviour implies that evaporation of any remaining volatile component (e.g. H_2O, B_2O_3) is zero or rather small (less than resolution limit of the TG system) at 700 °C.

In other test series with a change from dry to wet gas conditions a fast mass increase was detected at low temperatures which was correlated with a fast H_2O absorption by the B_2O_3 powder and formation of boric acids. This effect was found to be reversible.

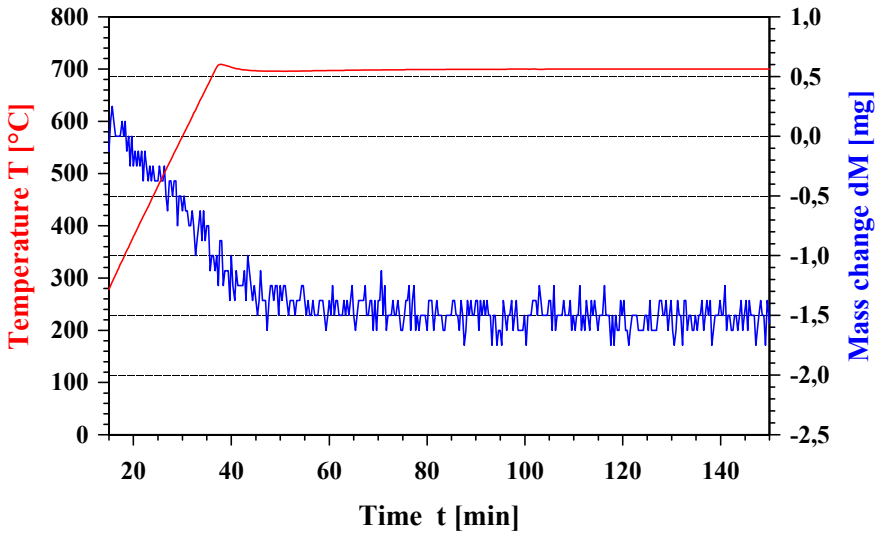

Fig. 6: Dried B_2O_3 sample mounted in the DTA-TG-system under air and heated to 700 °C under flowing Argon. Mass of powder 127 mg.

4.3 Behaviour of B_4C under inert conditions

B_4C pellets (ESK and Framatome) and powders were analysed by TG tests under inert atmospheres (Ar) and transient heating to 700 °C. As can be seen from Fig. 7 a mass loss of up to 1.7 % was detected starting near a sample temperature of 200 °C. From this temperature evaporation of absorbed H_2O can be excluded and the mass loss has to be linked to evaporation of boric acids, which are present at the surface of the delivered samples.

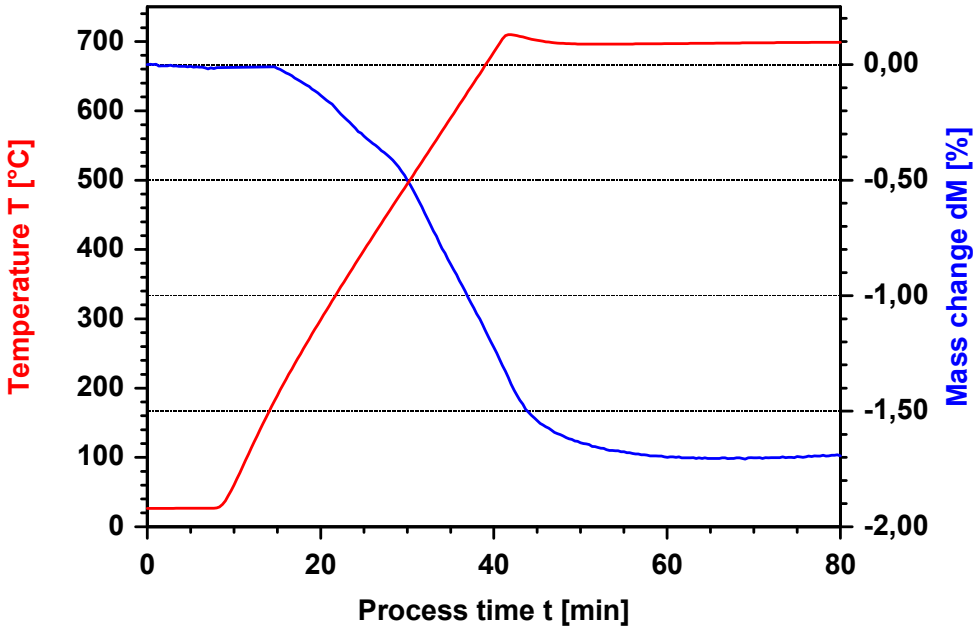

Fig. 7: Mass loss of B_4C during annealing in Ar atmosphere

4.4 Behaviour of B_2O_3 in dry and wet Ar atmosphere:

TG analyses of B_4C oxidation provide mass change data. The registered mass change is the sum of B_2O_3 formation minus B_2O_3 evaporation and C losses by formation of volatile C compounds. To separate these effects B_2O_3 evaporation rates have to be known. Evaporation rates were detected by evaporating B_2O_3 out off Y_2O_3 crucibles in the TG system in the temperature range 700 to 1300 °C. The atmosphere conditions were pure dry flowing Ar and H_20 saturated Ar produced by bubbling of Ar through a temperature controlled water bath. Measurements performed at 800 °C under flowing dry Ar showed (Fig. 8), that evaporation of B_2O_3 is rather small and can be neglected at that low temperature during B_4C oxidation in Ar-O_2. The mass loss in dry Ar atmosphere increases with temperature as can be seen from the slopes of the mass curve for the 900 and 1000 °C tests.

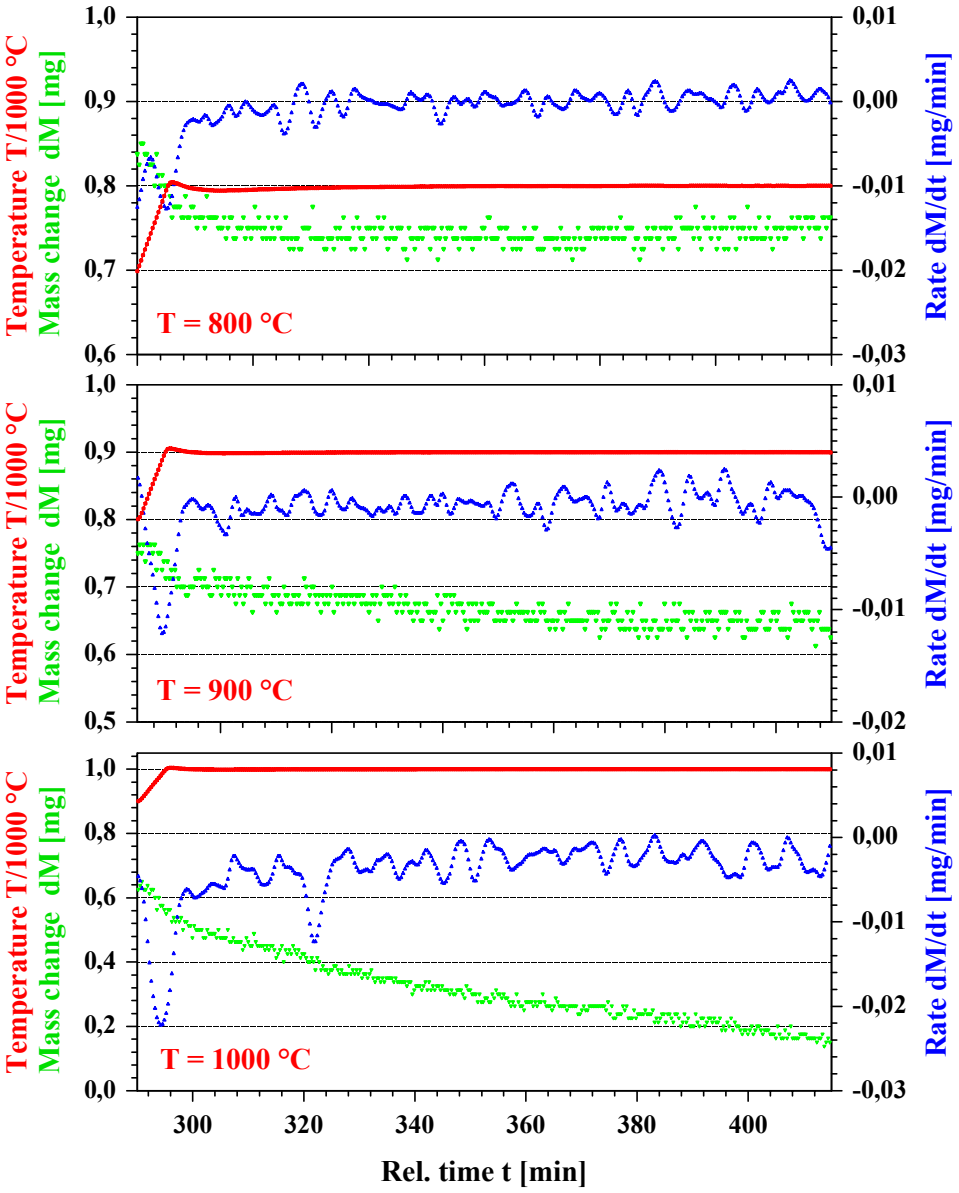

Fig. 8: Evaporation of B_2O_3 in dry flowing Ar atmosphere in dependence of temperature. Flow rate 10 l/h

Evaporation of B_2O_3 increases, if the carrier gas contains humidity. This can be correlated with the formation of boric acids whereby the biggest effect may come from H_3BO_3. For illustration of the increased evaporation by humidity a comparison is given in Fig. 9 for behaviour at 1000 °C and flow rate of 10 l/h. In Ar-steam mixture realized by saturation of Ar in a water bath at 20 °C the evaporation of B_2O_3 is about twice the effect detected in dry atmosphere. Experiments of this type were performed for different flow rates and partial pressures of steam. Ar saturation at 20 °C corresponds to a steam pressure of about 12 mbar under the actual test conditions. The 60 °C saturation leads to a pressure of about 100 mbar at sample position. The results of the tests are given in Fig. 10. Evaporation rate increases with temperature and is characterized by a line in the Arrhenius plot in the shown temperature range. Higher flow rates as well as increased humidity cause faster evaporation of B_2O_3.

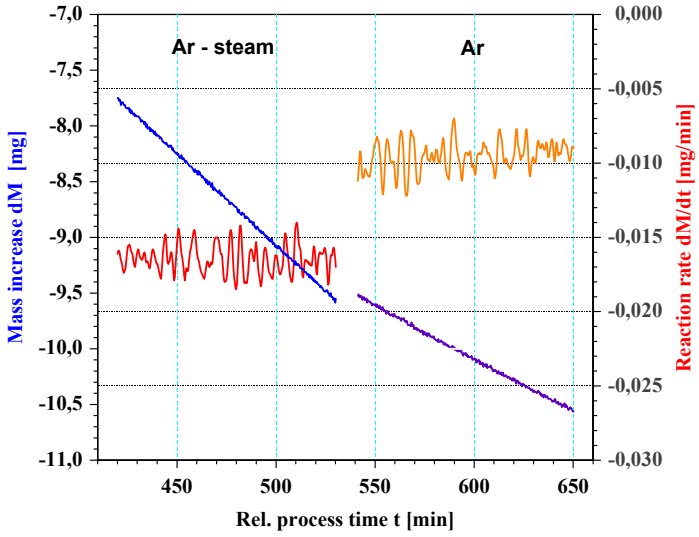

Fig. 9: Evaporation of B_2O_3 in flowing dry and wet Ar at 1000 °C

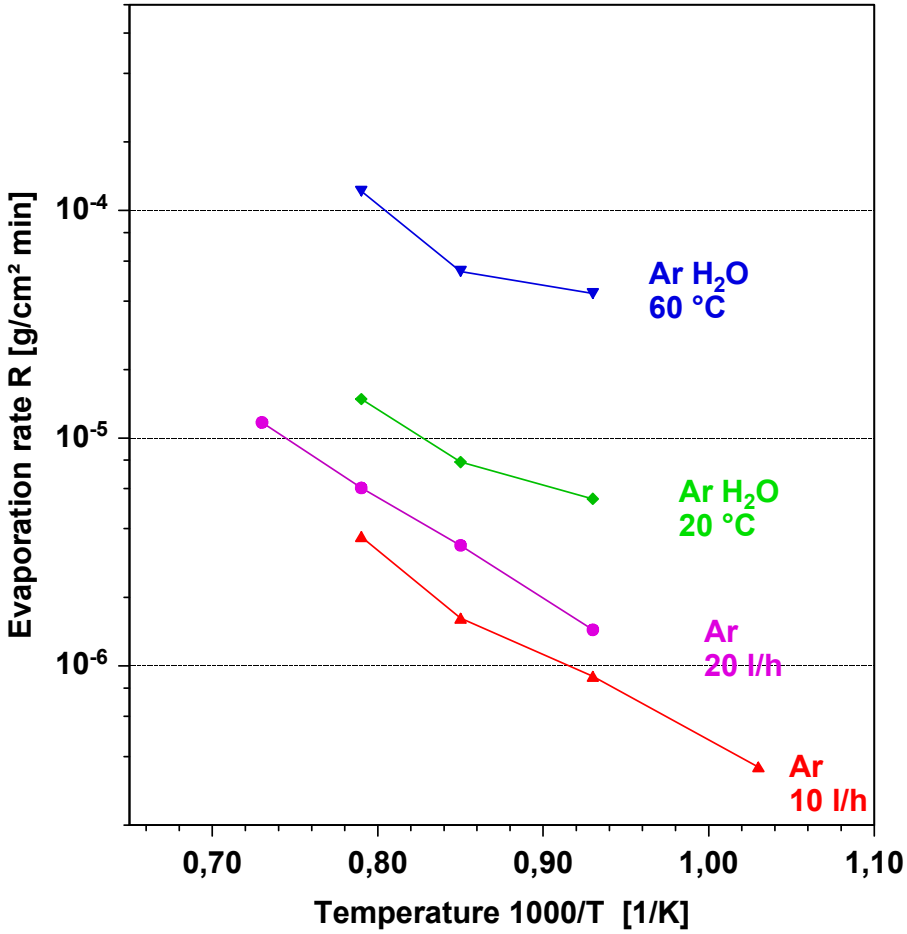

Fig. 10: Evaporation of B_2O_3 in dependence of flow rate (10 or 20 l/h) and steam concentration (12 or 100 mbar H_2O in 20 l/h Ar)

4.5 Behaviour of dense B_4C pellets in dry Ar/O_2 and wet Ar atmosphere:

Oxidation behaviour of dense B_4C pellets was examined in the temperature range between 700 and 1300 °C under flowing gas atmospheres. Extremely non prototypical experiments in Ar/O_2 atmosphere were chosen to study the B_2O_3 scale formation without the effect of boric acid formation and to separate counteracting mechanisms. An additional argument for this foregoing was the observed complex behaviour in mass change during first screening oxidation tests of B_4C. Three zones, as indicated in Fig. 11, with different mass change characteristics in dependence of time and varied temperature conditions could be observed. The detected mass decrease in zone 1 can be correlated with cleaning effects of the pellet during heating. Oxidation effects take not place in the resolution range of the TG system. In the temperature range from 600 to 1200 °C (zone 2) a mass increase during oxidation is present. The mass increase rates depend on time and temperature. At higher temperatures (zone 3) mass losses during test execution are observed. Special tests with isothermal conditions after transient test initiation were performed to determine the mechanisms and kinetics of the reaction processes leading to this complex picture.

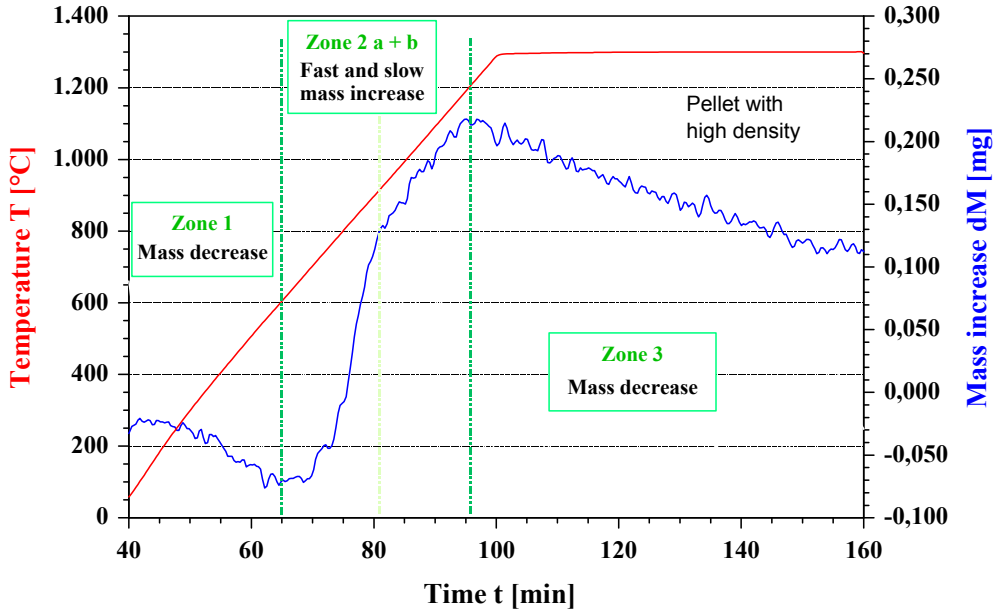

Fig. 11: Mass change behaviour during oxidation of dense B_4C pellet in Ar/O_2 atmosphere, flow rate 10 l/h.

Low temperature tests were chosen to study the scale formation without significant influence by B_2O_3 evaporation effects. As optimal reaction condition 800 °C was selected due to:

- Most part of volatile contaminations in B_4C pellets ranging from fabrication and handling are driven out at about 600 °C.
- First rather small mass increases were detected during transient heating with 20 K/min at about 620 °C
- Significant B_2O_3 formation in $Ar\text{-}O_2$ atmosphere of ratio 80 to 20 starts at about 650 °C.

The test (Fig. 12) was performed with a dense B_4C pellet, which was cleaned by annealing in vacuum at 700 °C before mounting into the thermal balance system. The total surface of the pellet with density 2.48 g/cm² was 6.51 cm² (Ø = 10.51 mm, h = 14.50 mm) whereby the exposed area was 5.7 cm². In the shown diagram without base line corrections first slow oxidation was detected at about 625° C during the transient phase to test temperature 800 °C. The mass increase during the heating up phase is about 1.1 g or roughly 10% of the total mass increase during the test time of 4 h. The time required for crossing the temperature range 600 to 800 °C was 10 min. The observed mass increase represents the oxygen uptake by formation of B_2O_3 minus the mass loss of carbon coming from formation of volatile CO_x compounds under the assumption that B_2O_3 losses by evaporation are small. The mass curve shows clearly that the oxidation process is slowed down during the test duration. Formation of a protective scale takes place. Parabolic reaction kinetics may be present, e.g. if the reaction is only diffusion controlled and no rearrangement of the scale takes place during the test.

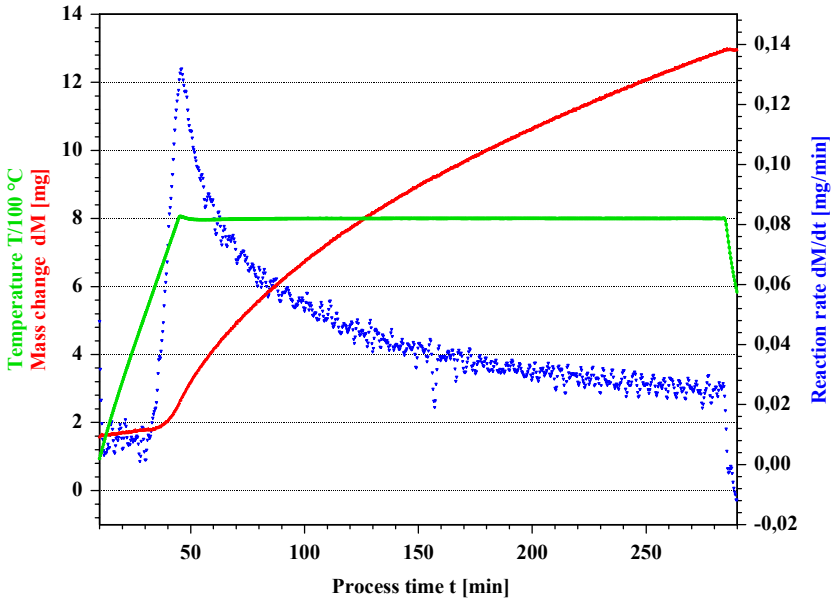

Fig. 12: Oxidation behaviour of B_4C in dry flowing Ar/O_2 atmosphere.

At higher temperatures evaporation of B_2O_3 increases and should lead to a clearly visible effect – e.g. deviation from the observed parabolic similar oxidation kinetics at 800 °C - in reaction behaviour of B_4C oxidation. In contrast to the expected mass losses caused by B_2O_3 evaporation and reduced reaction rates coming from a growing scale a continuous mass increase was observed as can be seen from Fig. 13. Post test inspection of the samples (Fig. 14) showed, that the formed oxide was flowing down and was accumulated on top of the sample support. Additionally to this effect during isothermal test condition changes appeared in reaction rate during heating up. These changes can only be explained if structural changes of the passivating scale take place and lead to higher O_2 diffusion e.g. by scale thinning and droplet formation.

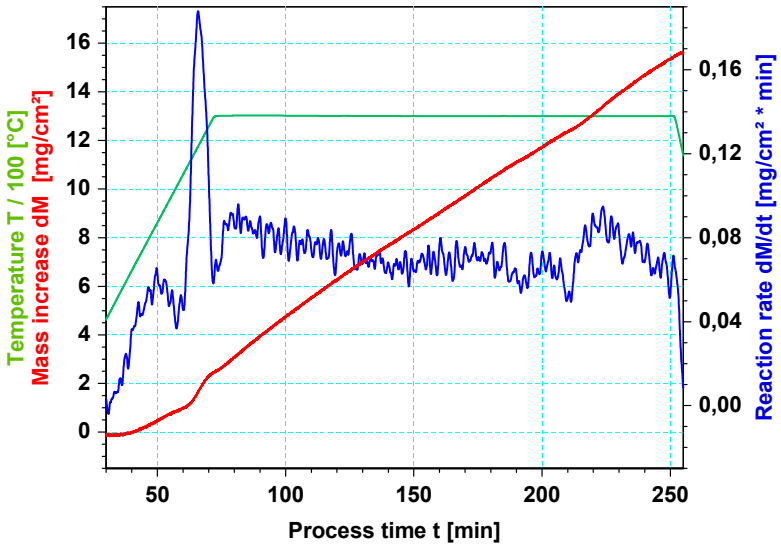

Fig. 13: Flow down of formed oxide scale. Dense B_4C oxidized at 1300 °C in Ar-O_2 atmosphere.

Fig. 14: Flow down of oxide scale. The sample support is covered by a glassy B_2O_3 skin

In comparison to the oxidation of B_4C pellets in dry Ar-O_2 atmosphere a modified mass change behaviour was expected for the reaction in steam saturated Ar gas. Oxidation tests with dense pellets were performed in the temperature range 800 to 1300 °C. The heating rate in the transient initiation phases of the isothermal tests was 20 K/min.

The mass change diagram of a test carried out at 800 °C is given in Fig. 15. The global behaviour of the mass change is similar to the oxidation tests done in Ar-O_2 atmosphere. Reaction rate increases first strongly and reaches a maximal value of about 0.14 mg/min in the transient phase. After that position the rate decreases continuously. The sample shows over the whole test period of about 5 h a steady mass increase.

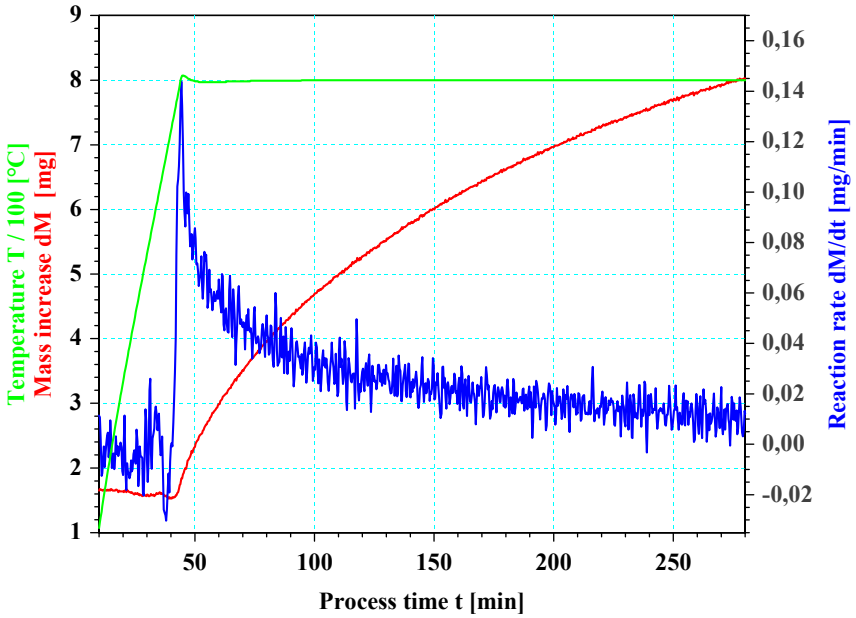

Fig. 15: Oxidation of a dense B_4C pellet in Ar-steam at 800 °C
Partial pressure: 12 mbar H_2O, Active surface: 5.7 cm²

However, at higher temperatures (1000 °C) as depicted in Fig. 16 the global behaviour changes. After a certain time a maximum in mass increase is reached, in this test short time after entering the isothermal test phase. For long test times mass loss dominates the reaction behaviour and is constant. The view on the sample after exposure to Ar-steam is given in Fig. 17. The surface of the pellet is covered by a glassy and transparent scale. Some small white pixels are present, which can be correlated with a reaction of B_2O_3 with steam.

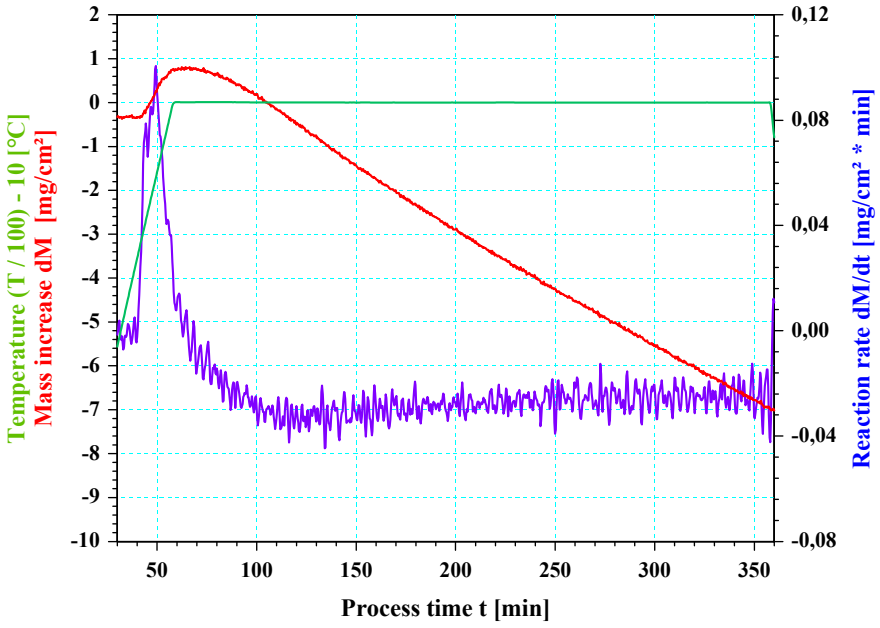

Fig. 16: Oxidation of dense B_4C at 1000 °C in
Ar-steam atmosphere

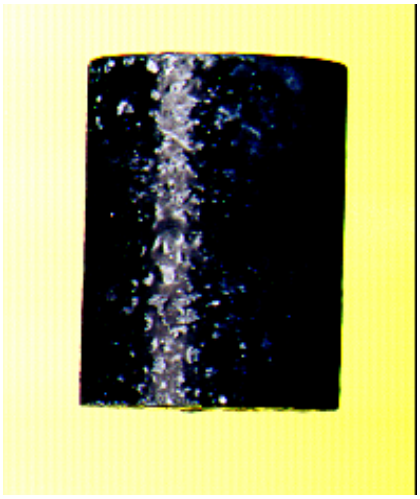

Fig.17: Dense B_4C pellet after exposure to Ar-steam at 1000 °C

For higher test temperatures the maximum in mass gain was reached already in the transient heat up phase (Fig. 18). Also it can be seen that reaction rates increase with temperature. Furthermore, reaction rates depend also on flow rate (constant partial pressure) as can be seen from Fig. 19.

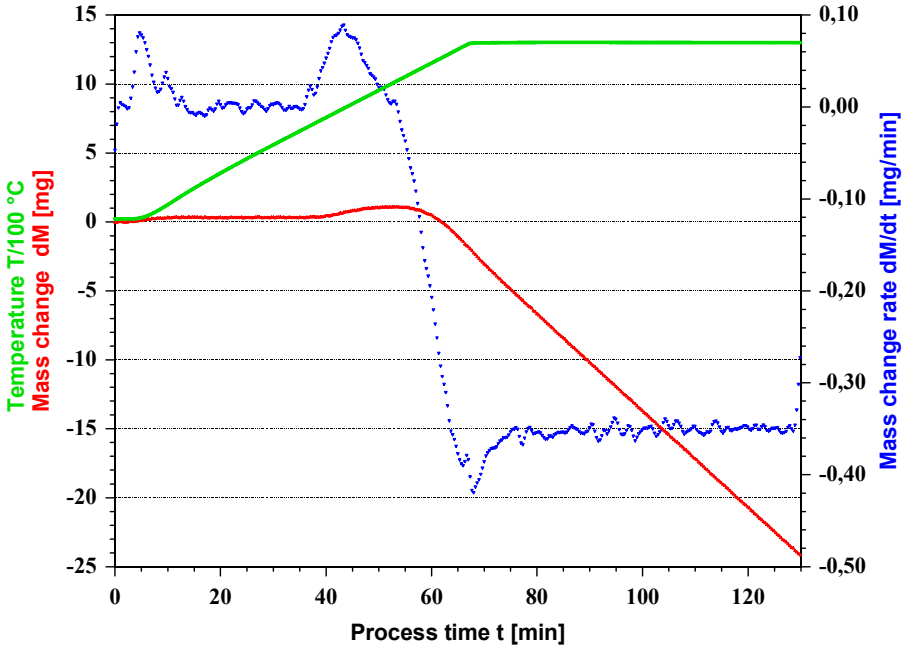

Fig. 18: Oxidation of a dense B_4C pellet in Ar-steam at 1300 °C
Flow rate 20 l/h, partial pressure 100 mbar H_2O
Active surface 5.7 cm²

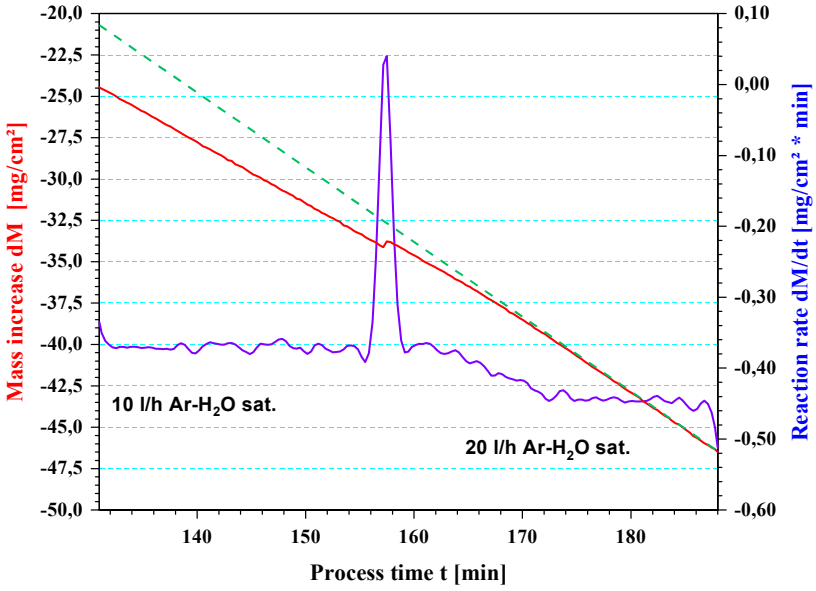

Fig. 19: Influence of flow rate on evaporation / reaction rate at 1300 °C in Ar-steam atmosphere

In contrast to the B_4C oxidation in dry Ar-O_2 atmosphere equilibrium conditions could be observed in the isothermal test phase during tests in Ar-steam atmosphere. The scales are thin enough so that B_2O_3 formation is equal to evaporation. For long test duration formation of new B_2O_3 is constant and equal to the evaporation of B_2O_3. The reaction is governed by diffusion controlled oxidation with parabolic kinetics and linear kinetics in evaporation.

4.6 Behaviour of porous B_4C pellets in dry Ar/O_2 and wet Ar atmosphere:

Reactor typical B_4C pellets (Framatome) have a density of about 71 % TD. By this fact additional reaction mechanisms are expected. Typical values of these pellets are: Mass = 1.107 g, Size: H x D = 14.30 x 7.47 mm, Density 1.80 g/cm³. The active surface of the samples for studying the reaction behaviour was roughly 3.73 cm². Fig. 20 depicts the mass and rate curves for a test done at 800 °C in Ar-O_2 atmosphere. Under these conditions the global reaction behaviour of the porous pellet is similar compared to the curves taken from dense pellets. This means, that a steady mass increase over the whole test period of about 6 hours is present and the rate decreases with time.

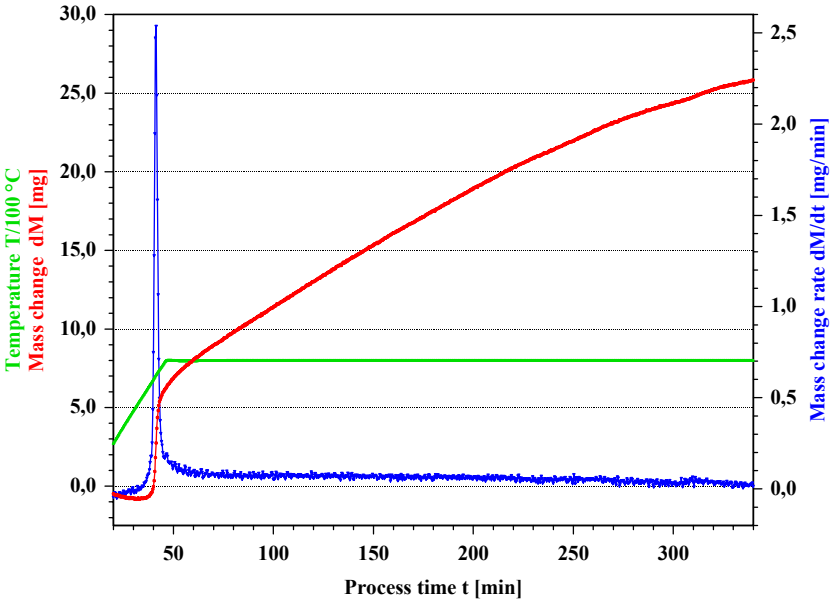

Fig. 20: Oxidation of porous B_4C pellet in Ar-O_2 at 800 °C

At higher temperatures (Fig. 21, 1000 °C) the shape of the mass curve for oxidation in Ar-O_2 atmosphere does not change drastically. This means a steady mass increase occurs during transient heat up phase and isothermal test period. However the rate curve indicates by their structuring in the low temperature range (800 to 1000 °C), that additional mechanisms compared to continuous and steady scale growth have to be present. A possible explanation for the second maximum of the rate curve near 980 °C may be found in the higher mobility of the formed oxide together with a filling of pores. This process would lead to a scale thinning at the active surfaces and an increase in rate under the boundary condition that mass increases also.

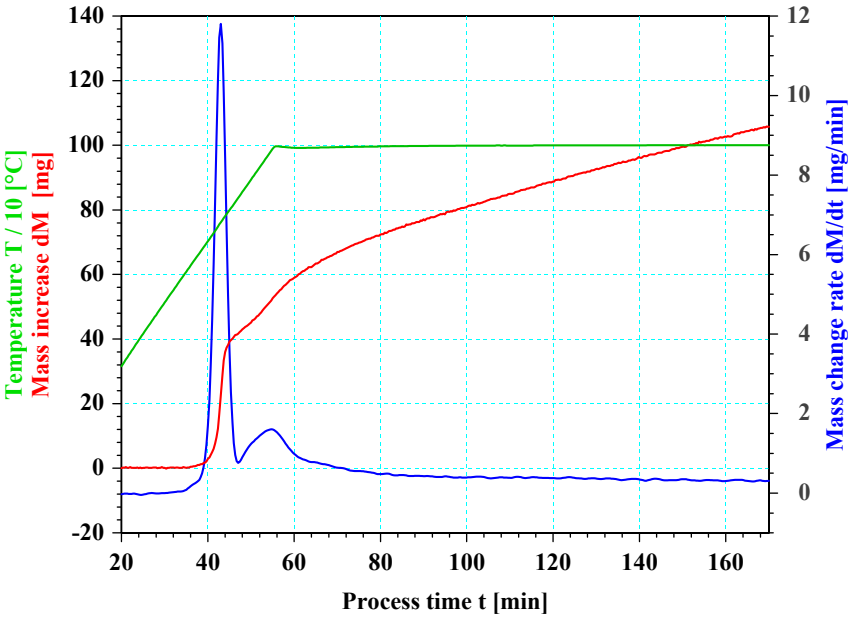

Fig. 21: Oxidation of porous B_4C pellet in Ar-O_2 at 1000 °C

In wet Ar atmospheres the general shape of the mass curve changes compared with curves observed in dry Ar-O_2 oxidation tests. After a certain time a maximum in weight gain is reached caused by fast oxide formation and still missing protective scales. Later on mass loss is registered. For TG tests at 1000 °C the maximum in weight is reached about 40 min after entering the isothermal test phase (Fig. 22). The test conditions were 20 l/h Ar and a steam content of 12 mbar. Heating rate was 20 K/min.

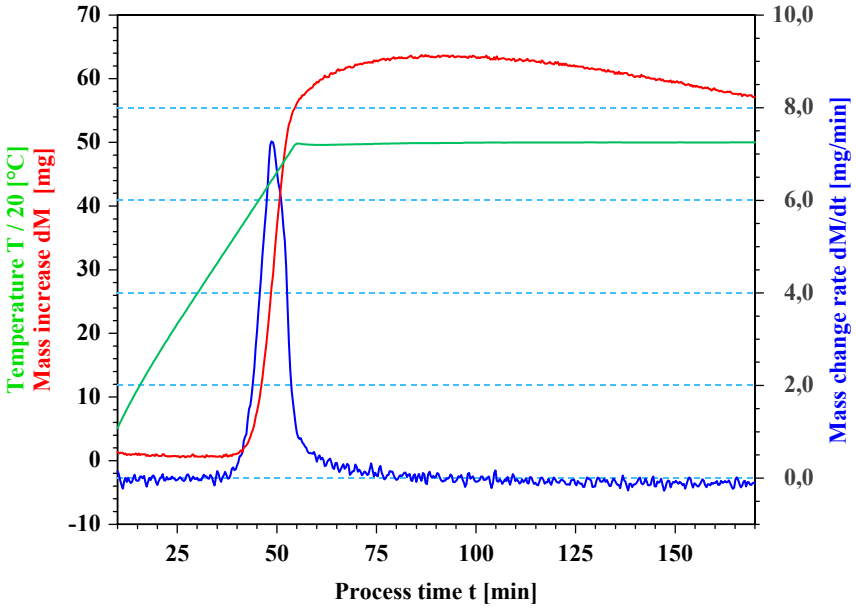

Fig. 22: Oxidation of porous B_4C pellet in Ar-steam at 1000 °C

Tests with fast temperature changes e.g. from 1000 °C to 1100 °C (Fig. 23) showed that the evaporation (mass losses) depends on temperature.

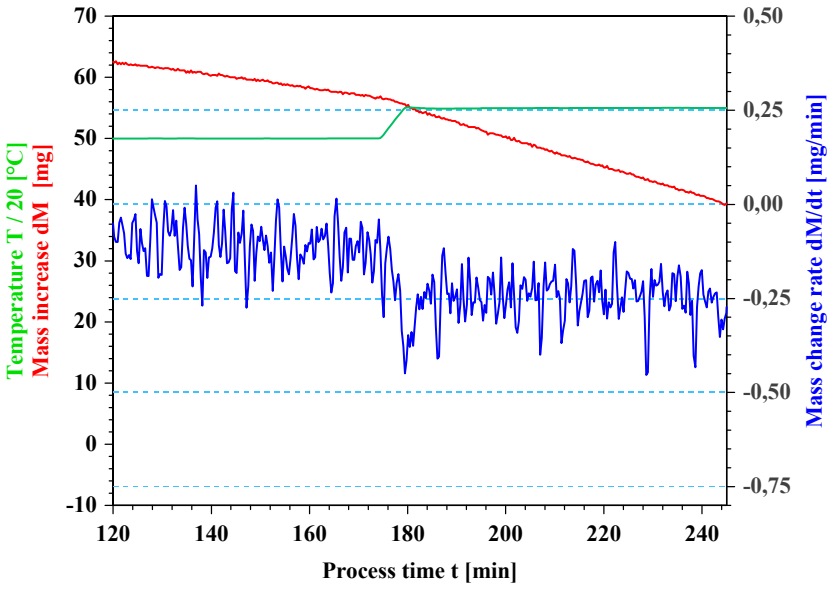

Fig. 23: Mass loss increases with a fast temperature step from 1000 to 1100 °C under Ar-steam atmosphere

A temperature increase of 100 K before crossing the maximum in weight gain leads to a sharp change in reaction rate from positive to negative slope as depicted in Fig. 24. A change from Ar-steam to Ar eliminates oxidation and allows only evaporation. The mass loss indicates that volatile components were present. Under the assumption that B_2O_3 is this species the detected mass loss corresponds to a scale thickness of about 0.8 µm. However, it is not necessary that all the present amount of volatile components evaporated in the registered time period.

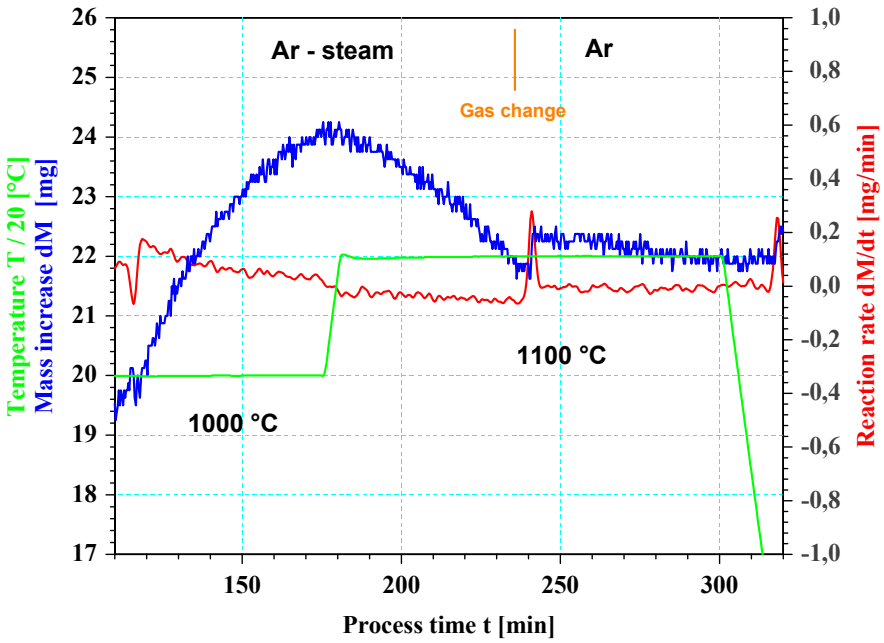

Fig. 24: Oxidation test of reactor grade B_4C pellet at different temperatures and under atmosphere changes Ar-H_2O(12 mbar) to Ar

4.7 Comparison of porous vs. dense B_4C pellets:

Some specific tests are selected to show common features in reaction behaviour of dense and porous pellets. In Fig. 25 a comparison is given for the reaction of reactor grade pellets vs. dense B_4C pellets. Both materials show mass increase at 800 °C during 4 h test duration. For both pellet types evaporation losses are smaller than weight gains by oxidation. However the mass increase of the reactor grade B_4C pellet is about 30 times that of dense pellets for the given test time. The biggest differences in mass increase occur in the beginning of oxidation and the scale formation process. The enhanced reaction rate is due to the enlarged active surface of the porous material. For long test durations reaction rates of both materials are similar and indicate that passivation takes place.

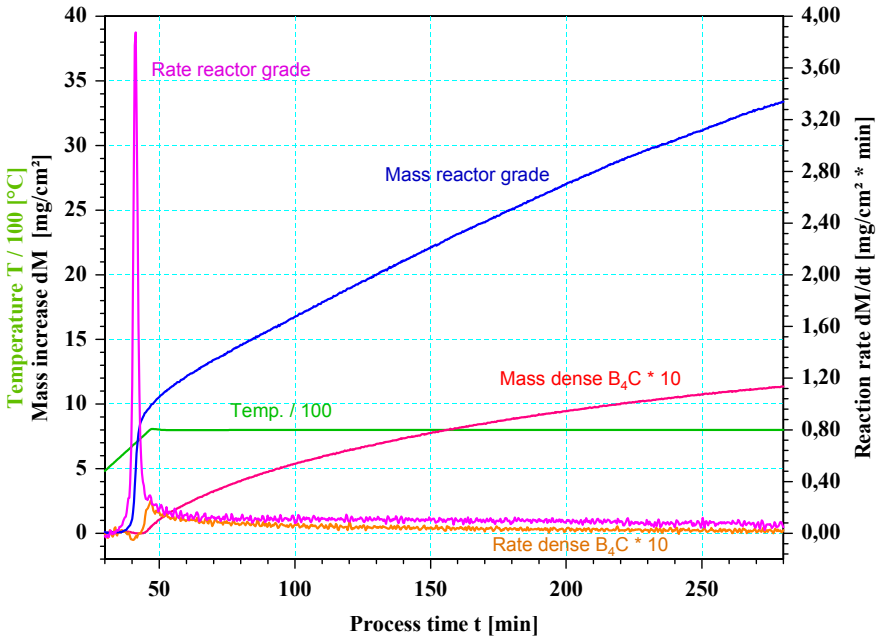

Fig. 25: Comparison of reaction behaviour for dense vs. reactor grade B_4C at 800°C in Ar steam. Partial pressure 100 mbar

For higher temperatures a maximum in weight gain is reached in the chosen test duration as can be seen in Fig. 26. After that time pellet mass begins to decrease by evaporation of boric acid in the Ar-steam flow and reduced B_2O_3 production. Short time later an equilibrium occurs between evaporation and oxidation. The thickness of the formed active oxide scale is then constant.

A flow down of the melt was not observed for tests performed in Ar-steam atmospheres by post test analyses. However, the surfaces of the reactor grade pellets were rough and had no uniform surface structure Fig. 27.

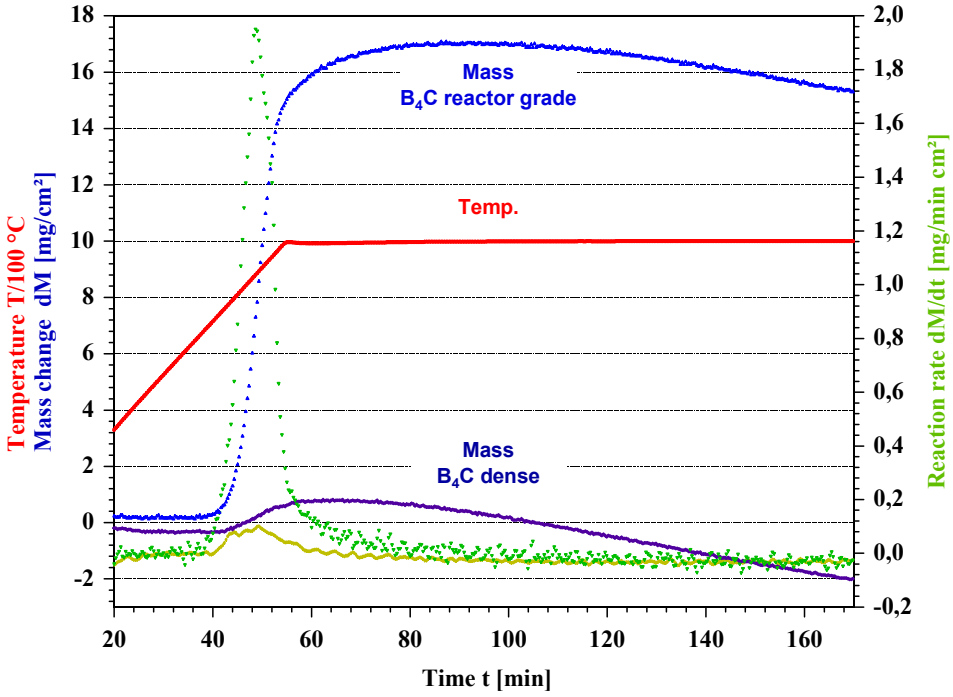

Fig. 26: Oxidation of B_4C pellets in Ar-steam at 1000 °C, partial pressure 100 mbar.

Fig. 27: Porous B_4C pellet after test in Ar-steam (1100 °C)

5. Approach for evaluation of B_4C tests and their modelling:

The analyses of the TG tests showed early that an evaluation towards B_4C oxidation kinetics and comparison of data sets coming from different test equipments will be rather hard or impossible without modelling support. To provide oxidation relevant evaluated data two independent modelling approaches were started and included into the SET program. Both were focused in the first stage of development to interpret / evaluate the TG test data performed on dense pellets. In next steps the models will be applied to other test methods and reactor typical porous B_4C pellets.

Both modelling approaches started with the common assumption, suggested by the shape of the TG mass curves detected during reaction of dense pellets, that a passivating scale is first formed on the B_4C pellets within the tested temperature range and as a second process evaporation of the formed oxide takes place. In the first test runs it was assumed for simplification that the evaporation may only depend on temperature. In next steps a more complex dependency (e.g. gas velocity, steam concentration) was integrated.

<u>BORCA model to evaluate oxidation of high density material</u>

The first approach was based on assuming parabolic B_2O_3 scale growth and linear B_2O_3 evaporation in dry Ar-O_2 atmosphere. The following balance equation was used:

$$\frac{dm^{ox}}{dt} = \frac{a}{m^{ox}} - b$$

$m^{ox} = \rho^{ox}\delta^{ox}$ is the specific mass of the oxide film

The rate parameters a and b have to be determined with the help of the experimental data.

For the first qualification a TG test performed in dry Ar-O_2 at 800 °C was selected. Under this condition the parameter b could be neglected and set to zero as a result of the B_2O_3 evaporation tests.

By fitting the mass change curve (Fig. 28) the parameter a was determined to:

$$a = 0.102 * 10^{-3} \exp(-1.298 * 10^{4}/T)$$

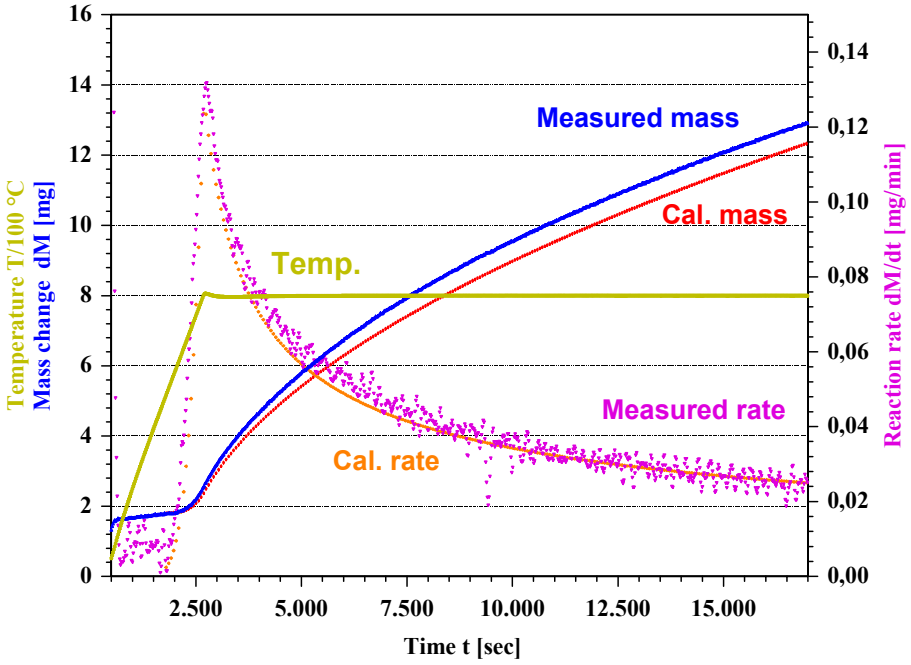

Fig. 28: Modelling approach for TG oxidation test of dense B_4C in dry Ar-O_2 atmosphere at 800 °C

Under the assumption that the determined parameter a (Ar-O_2 atmosphere) is also valid for Ar-steam oxidation tests modelling was extended to reactions in wet Ar atmospheres. Fig. 29 shows the comparison of a thermo-balance test and the modelling by BORCA [4].
The parameter b was determined to $b = 9.612 * 10^{-4} \exp(-5.19 * 10^{3}/T)$

The mass evolution could be simulated in good agreement to the TG test and a thickness of the protective scale in dependence of the test time was calculated. During the isothermal test phase the scale thickness is constant. An equilibrium in formation and evaporation of B_2O_3 is present.

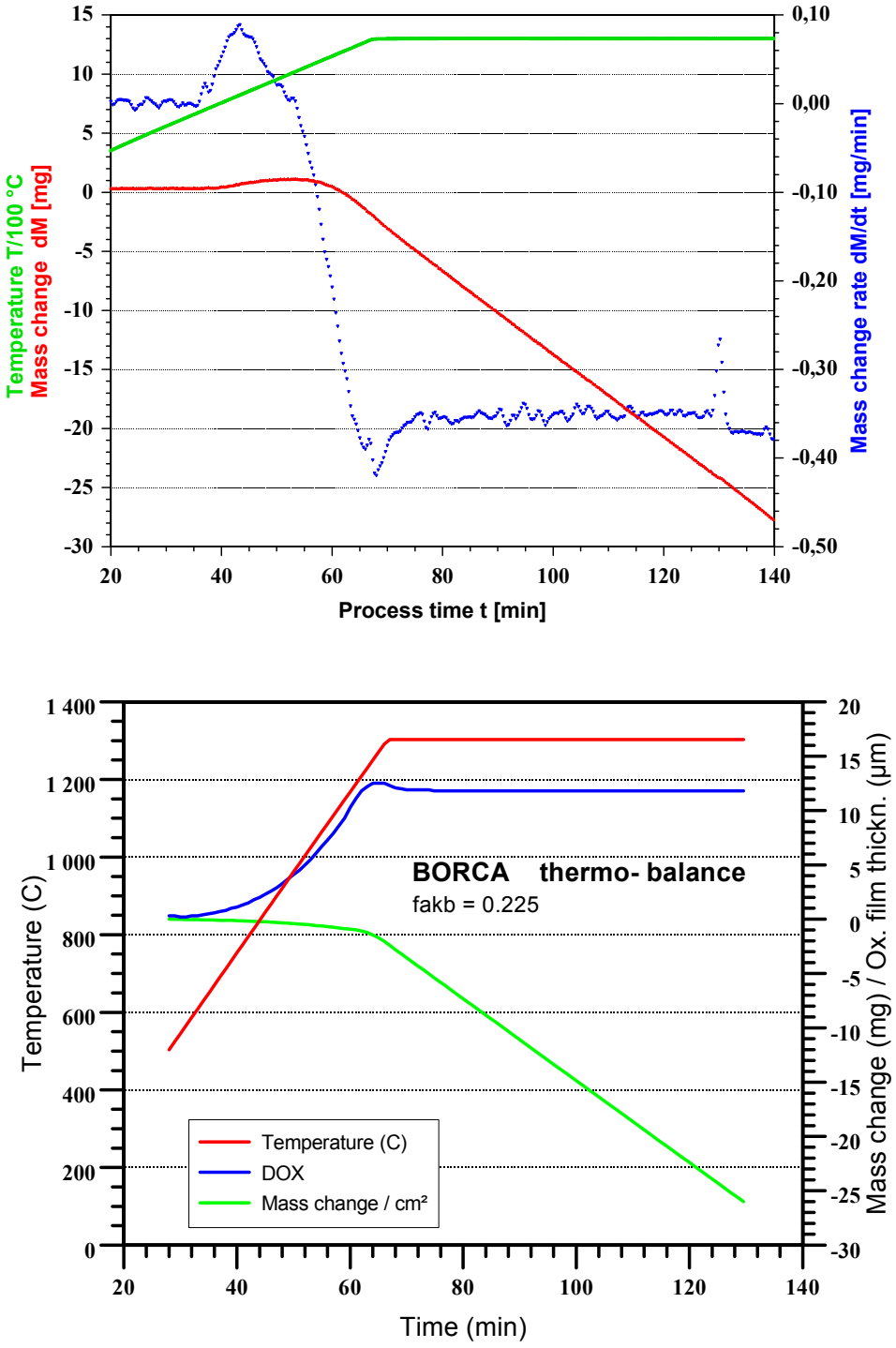

Fig. 29: Simulation of a TG oxidation test of dense B_4C in Ar-steam at 1300 °C

With the second approach a direct evaluation of each test was aspired. This means that no intermediate evaluation e.g. of the parabolic rate coefficient k_p has to be done by evaluation of an other specific test with r = 0 or negligible for the linear evaporation rate. The applied correlation for scale growth was:

$$\frac{dx}{dt} = \frac{k_p}{x} - \frac{\mathrm{r}}{\rho_p}$$

The parameters k_p and r can be fitted by an iteration procedure using the experimentally determined mass change and rate data.

This evaluation technique was tested with several TG tests. Fig. 30 shows the result for an Ar-steam test. The analysis, applied for the isothermal phase, can reproduce the maximum in weight gain and the mass losses by evaporation. Beyond the fitting of the curves, which is sensitive to correctly extracted mass change and rate data, B_2O_3 scale growth and B_4C consumption can be predicted (Fig. 31).

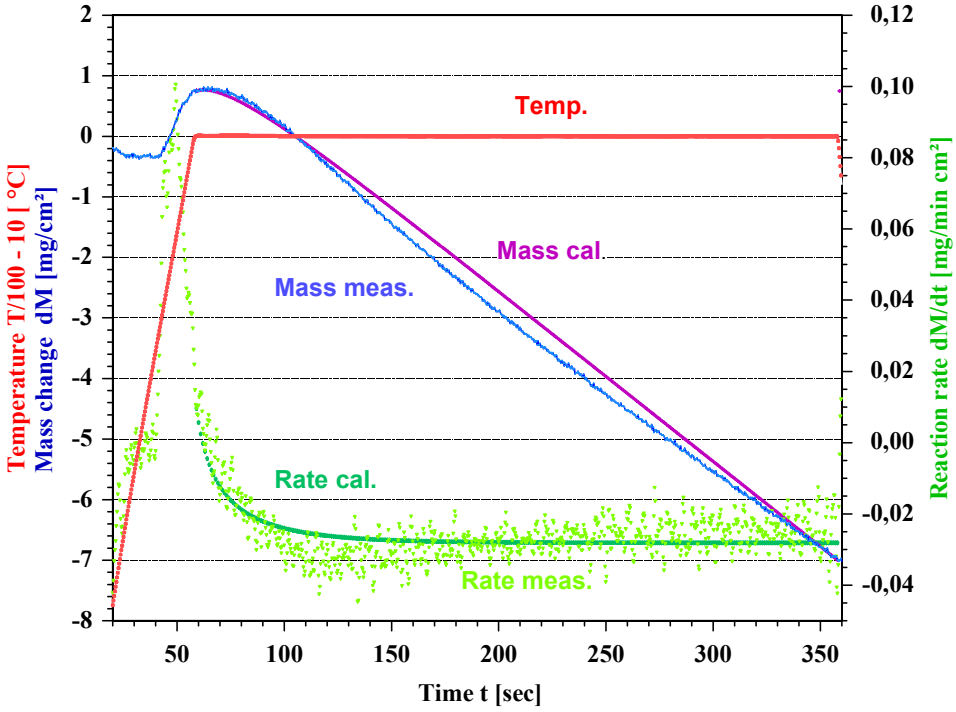

Fig. 30: TG test of dense B_4C in Ar-steam
at 1000 °C, 20 l/h Ar, 100 mbar H_2O
Comparison test vs. analysis

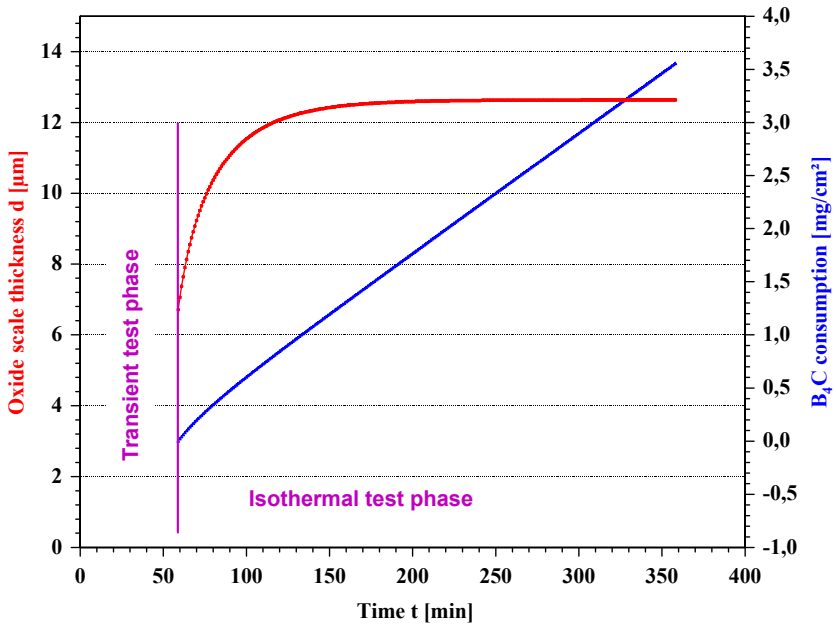

Fig. 31: Calculation of B_2O_3 scale growth and B_4C consumption for the test performed at 1000 °C

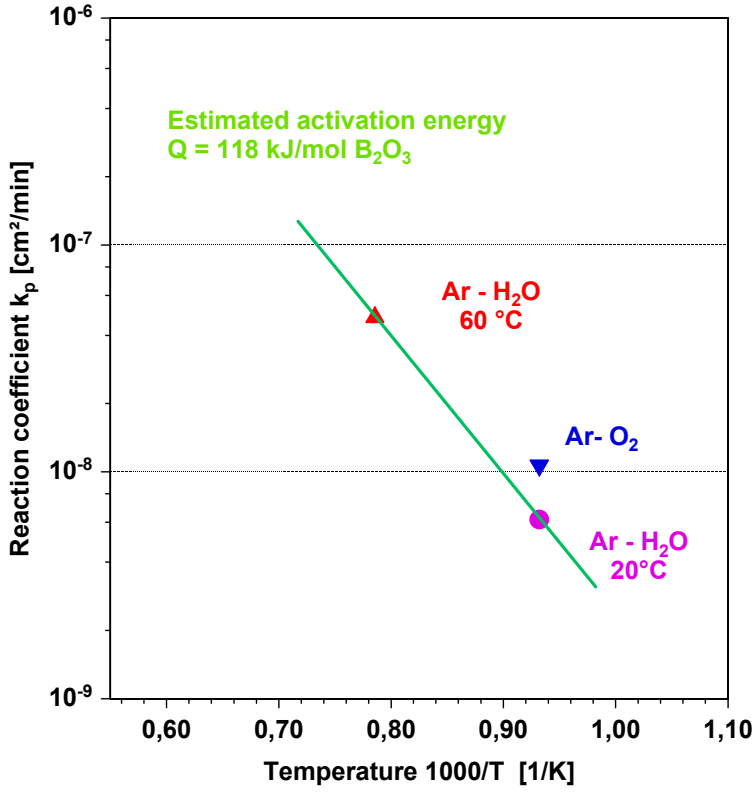

Fig. 32: Parabolic rate coefficient k_p for B_2O_3 scale growth and estimation of activation energy for B_2O_3

6. Concluding remarks to TG B_4C tests and modelling

- The B_4C oxidation is much more sensitive to environment conditions compared e.g. to Zry oxidation.
- Simple test conditions (not severe accident typical) are necessary to identify counteracting mechanisms for determination of reaction kinetics.
- In steam containing atmospheres the oxidation rate of B_4C is governed by the evaporation of B_2O_3, the formation of boric acid and the transport in the vapour phase.
- The TG and BOX tests [3, 4] show similar and consistent reaction behaviour.
- Both SET methods are necessary by providing complementary results and a broader data base.
- Some of the occurring reaction mechanisms could be identified and separated.
- Modelling support is necessary for determination of reaction kinetics parameters and for verification of mechanisms.
- First modelling tools were developed and can describe, both, TG and BOX results.
- The inclusion of modelling efforts, performed in parallel to the experimental programs, has contributed to an advanced interpretation of the phenomena and the determination of the kinetics data.

The performed SET's provide a base for interpretation of mechanisms occurring during B_4C oxidation. Furthermore, thermo-dynamical reaction parameters (e.g. parabolic rate coefficient or activation energies) can be determined and different kinds of tests (TG or BOX tests) deliver a consistent picture. However, the quantification of the effects and parameters have to be seen as preliminary. An intense verification process has to follow, independently and also beyond COLOSS cooperation, to define parameter values with sufficient accuracy. Additional modelling efforts will be necessary to support data evaluation and to quantify environmental effects on B_4C oxidation as well as to integrate this knowledge into bundle test interpretation, code development and severe accident risk assessment.

Appendix A:

Preliminary state of interpretation of B_4C oxidation:

A-1 Evaluation approach

An evaluation towards B_4C oxidation kinetics parallel to the experiments was necessary for orientation and consistent analysis, especially of the evaporation tests performed with B_2O_3 melt. The approach, including not directly accessible parameters, is applied for the TG experiments as a first step, but application for other experimental results is possible.

The oxidation of boron carbide is assumed, firstly, to form a cover layer of boron oxide (B_2O_3) within the whole temperature range of actual interest. Secondly, the evaporation of B_2O_3 and the transfer of boric acid with steam per area and time span, respectively, shall proceed according to a not explicitly time-dependent rate r, which may be any function of temperature, atmosphere and flow conditions. Thirdly, the approach assumes that the reaction proceeds according to the geometrical surface area, which means a restriction to dense B_4C. A final assumption, plausible according to literature [5] and obtained TG results, is to fix the gross B_2O_3 layer growth as parabolic and the layer thinning as linear. Accordingly, a parameter k_p is defined as parabolic rate coefficient and a parameter r as linear evaporation rate. Densities and molar masses are given as ρ and M. The variables definition is as follows:

- The B_2O_3 layer grows with positive coordinate x as x(t), the index p indicates product.
- The B_4C specimen is consumed with the positive coordinate y as y(t), the index e indicates educt.
- The mass gain per unit surface area is m(t).
- The volume gain per unit surface area is v(t).

The resulting correlations for the scale thickness evolution and boron mass conservation (per area and time) are:

$$\frac{dx}{dt} = \frac{k_p}{x} - \frac{\mathrm{r}}{\rho_p} \qquad (8)$$

$$\frac{2\rho_e}{M_e}\frac{\mathrm{dy}}{\mathrm{dt}} = \frac{\rho_p}{M_p}\frac{dx}{dt} + \frac{r}{M_p} \qquad (9)$$

Mass gain and volume gain (both area and time reduced) proceed according to:

$$\frac{dm}{dt} = \rho_p \frac{dx}{dt} - \rho_e \frac{dy}{dt} \qquad (10), \text{ and}$$

$$\frac{dv}{dt} = \frac{dx}{dt} - \frac{dy}{dt} \qquad (11)$$

The four differential equations in common define the problem completely, if k_p and r are taken as known parameters for the given temperature. Eq. (8) defines the scale growth, Eq. (9) the boron carbide consumption, Eqs. (10) and (11) the mass and volume gain, respectively.

A-2 Combined differential equations and isothermally integrated forms

Various dependencies can be deduced from combinations of Eqs. (8) to (11), which are helpful for experiment interpretation (maxima of mass curves, initial volume gain as prediction of possible pore clogging effect, limiting dependencies towards short or long test duration). The straightforward isothermal integration of some equations is also useful. The most helpful ones are given here:

$$\frac{r^2 t}{\rho_p^2 k_p} + \frac{r(x-x_0)}{\rho_p k_p} + \ln\left|\frac{\rho_p k_p - rx}{\rho_p k_p - rx_0}\right| = 0 \qquad (12)$$

$$\frac{dy}{dt} = \frac{M_e}{2M_p}\frac{\rho_p}{\rho_e}\frac{k_p}{x} \qquad (15)$$

$$\frac{dm}{dt} = \rho_p\left(1 - \frac{M_e}{2M_p}\right)\frac{k_p}{x} - r \qquad (13)$$

$$m - m_0 = \frac{\rho_p\left(2M_p - M_e\right)}{2M_p}\left(x - x_0\right) - \frac{M_e r}{2M_p}t \qquad (14)$$

$$\lim_{t\to\infty}(x) = x_{stat} = \frac{\rho_p k_p}{r}\text{, or:} \qquad \lim_{t\to\infty}\left(\frac{dx}{dt}\right) = 0$$

$$\lim_{t\to\infty}\left(\frac{dy}{dt}\right) = \frac{rM_e}{2\rho_e M_p}, \quad \lim_{t\to\infty}\left(\frac{dm}{dt}\right) = -\frac{rM_e}{2M_p} \text{ and } \lim_{t\to\infty}\left(\frac{dv}{dt}\right) = -\frac{rM_e}{2\rho_e M_p} \quad \left(= -\lim_{t\to\infty}\left(\frac{dy}{dt}\right)\right)$$

A-3 Reduction of the formalism to interrelations between dimensionless auxiliary variables

The interrelations between the variables including ρ_p and k_p can be transformed to a more straightforward scheme by introducing dimensionless variables as follows. A dimensionless time τ and the dimensionless variables dX, dY, dM und dV are defined in analogy to the real ones:

$$d\tau = \frac{r^2}{\rho_p^2 k_p}dt, \quad dX = \frac{r}{\rho_p k_p}dx, \quad dY = \frac{r}{\rho_p k_p}dy, \quad dM = \frac{r}{\rho_p k_p}dm, \quad dV = \frac{r}{\rho_p k_p}dv$$

With those variables Eqs. (8) to (11) are transformed to equivalent ones, in which k_p and r do not occur any more:

$$\frac{dX}{d\tau} = \frac{1}{X} - 1 \qquad (8^*)$$

$$\frac{dY}{d\tau} = \frac{M_e}{2M_p}\frac{\rho_p}{\rho_e}\left(\frac{dX}{d\tau} + 1\right) \qquad (9^*)$$

$$\frac{dM}{d\tau} = \rho_p\frac{dX}{d\tau} - \rho_e\frac{dY}{d\tau} \qquad (10^*)$$

$$\frac{dV}{d\tau} = \frac{dX}{d\tau} - \frac{dY}{d\tau} \qquad (11^*)$$

$$\lim_{\tau\to\infty}(X) = 1$$

$$\lim_{\tau\to 0}\left(\frac{dX}{d\tau}\right) = \frac{1 - X_0}{X_0} \qquad \lim_{\tau\to\infty}\left(\frac{dX}{d\tau}\right) = 0$$

$$\lim_{\tau\to 0}\left(\frac{dY}{d\tau}\right)=\frac{M_e}{2M_p}\frac{\rho_p}{\rho_e}\frac{1}{X_0} \qquad \lim_{\tau\to \infty}\left(\frac{dY}{d\tau}\right)=\frac{M_e}{2M_p}\frac{\rho_p}{\rho_e}$$

$$\lim_{\tau\to 0}\left(\frac{dM}{d\tau}\right)=\frac{2M_p-M_e}{2M_p}\frac{\rho_p}{X_0}-\rho_p \qquad \lim_{\tau\to \infty}\left(\frac{dM}{d\tau}\right)=-\frac{M_e}{2M_p}\rho_p$$

$$\lim_{\tau\to 0}\left(\frac{dV}{d\tau}\right)=\frac{2M_p\rho_e-M_e\rho_p}{2M_p\rho_e X_0}-1 \qquad \lim_{\tau\to \infty}\left(\frac{dV}{d\tau}\right)=-\frac{M_e}{2M_p}\frac{\rho_p}{\rho_e}$$

Thus, the trends of all aspects of B_4C oxidation can be compared to those of the experimental results. With the introduced auxiliary variables this is possible without knowing the parameters k_p and r. Of course, the position within the dimensionless variables range remains unknown for the moment, as well as the size factor.

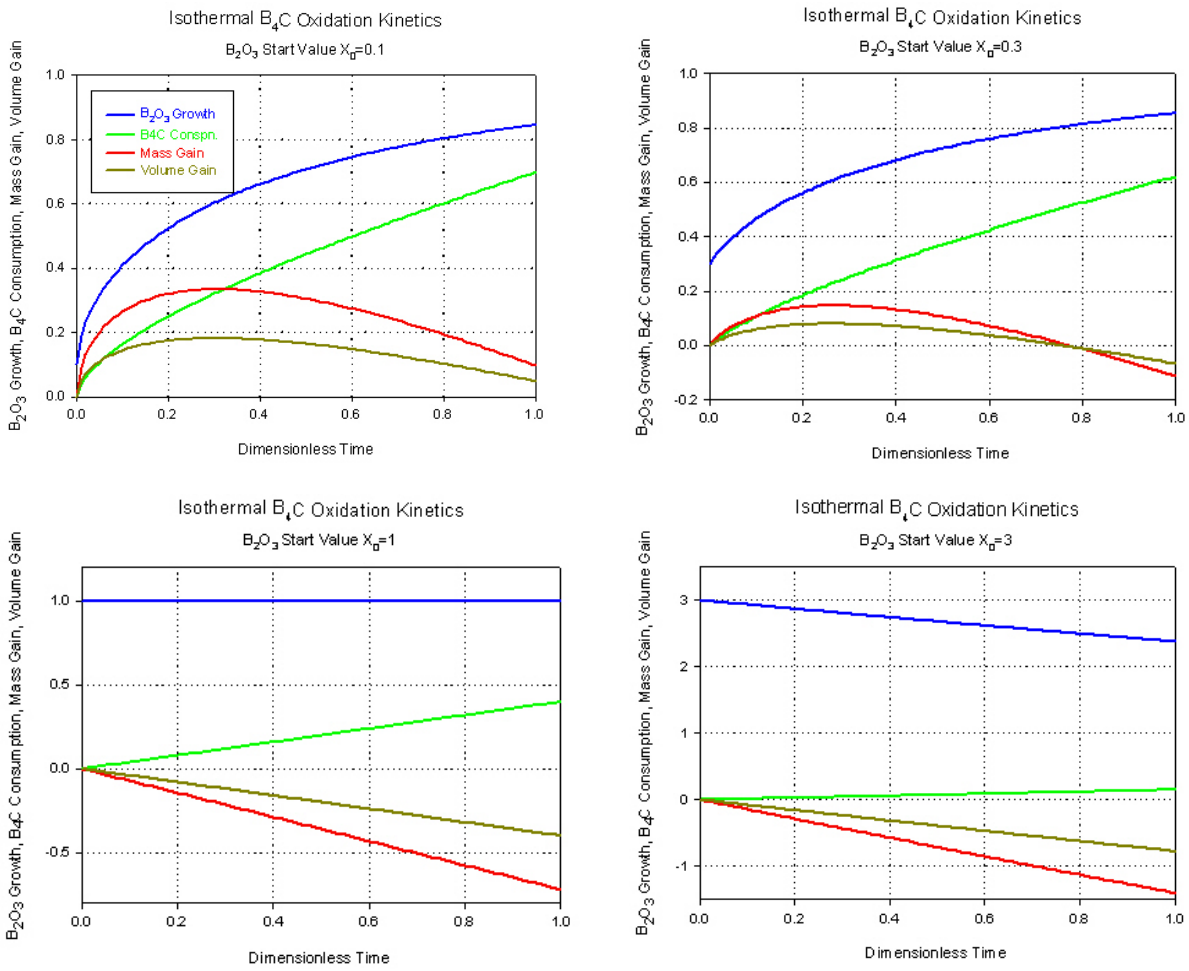

Fig. A1: Isothermal kinetic results in relation to assumed paralinear B_4C oxidation in dimensionless representation, given for different relative values of initial B_2O_3 layer thickness ($X_0=x_0/x_{stat}$), and showing the generally possible curve forms

The curves X(τ), Y(τ), M(τ) und V(τ) are shown for the start values X_0= 0.1, 0.3, 1 and 3 over the time range τ=0 to 1 (Fig. A1). (The values taken for the molar masses are M_e=4*10,81+12,011=55,251 and $2M_p$=4*10,81+6*16=139,24; the related factors resulted in $M_e/2M_p$=0,39680 and 1-$M_e/2M_p$=0,60320. The assumed densities ρ_e=1,8 g/cm^3 (B_4C pellet, 70% dense) and ρ_p=1,812 g/cm^3 (B_2O_3, glassy) gave ρ_p/ρ_e=1,00667 and $M_e\rho_p/2M_p\rho_e$=0,39945.)

Fig. A2 gives the rates of B_4C consumption (positive rate) and those of layer, mass and volume growth or decrease, respectively, for the same start values of B_2O_3 layer as in Fig. A1. For X_0<1 the absolute values of all rates decrease towards the stationary levels, for X_0=1 those constant values are shown. The case X_0=3, which describes the decrease of an excessively thick layer, e. g. formed under “dry” pre-oxidation conditions, illustrates the sluggish trends of the rates for this case. Special tests to this scenario were not performed, however the evaluation of the test with fast temperature increase shown in Fig. 24 underlines this behaviour as a tentatively realistic one.

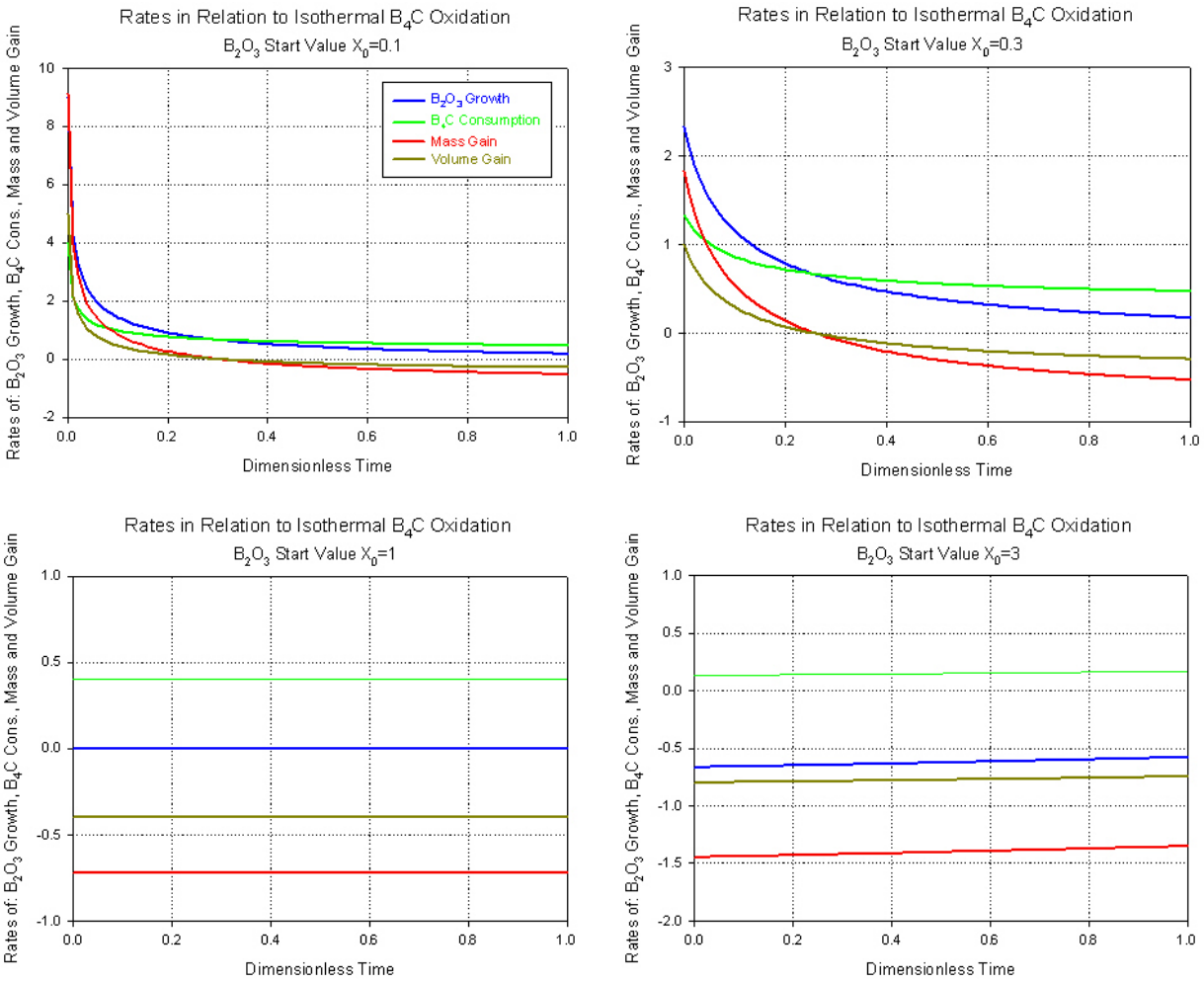

Fig. A2: Isothermal rates in relation to assumed paralinear B_4C oxidation in dimensionless representation, given for different relative values of initial B_2O_3 layer thickness ($X_0=x_0/x_{stat}$), and showing the generally possible curve forms

A-4 Determination of the parameters k_p and r by fitting to results of individual TG experiments

The derived formalism is applied to the evaluation of individual TG experiments, as long as the temperature dependencies of the parameters are not known, only for isothermal sections. The procedure is the following: In a first step the characteristics of the master curves for mass and mass change are compared to those of the experimental curves. Recognition of the correct curve form requires finding the adequate layer thickness values at start and end position of the corresponding scale growth curve. In a next step those values are taken to calculate the best-fitting parameters k_p and r, which is quite straightforward.

For the first step of the procedure the mass change rate and mass correlations (Eqs. 13 and 14) are used. Application to the start and end points of the experimental curves (indices 0 and 1) requires elimination of the unknown parameters k_p and r through replacing the real layer thicknesses by reduction to the stationary thickness $x_{stat}= \rho_p k_p/r$, using the factors α_0 and α_1: $x_0= \alpha_0 x_{stat}$ and $x_1= \alpha_1 x_{stat}$. Fitting to the experimental slopes s_0 and s_1 of the mass rate curve (setting $s_0=(dm/dt)_0$ and $s_1=(dm/dt)_1$) gives two equations and after mutual division the condition for the parameters α_0 and α_1:

$$\frac{(s_0 - s_1)\alpha_0\alpha_1}{s_0\alpha_0 - s_1\alpha_1} = 1 - \frac{M_e}{2M_p}$$

Similarly, inserting the experimental mass values and setting $m_0=0$, $t_0=0$, and $\Delta m=m_1$ and $\Delta t=t_1$ gives the condition for the parameters α_0 and α_1:

$$\frac{m_1\left(1 - \frac{M_e}{2M_p} - \alpha_1\right) + t_1 s_1 \alpha_1}{m_1\left(1 - \frac{M_e}{2M_p} - \alpha_1\right) + \frac{M_e}{2M_p} t_1 s_1 \alpha_1}(\alpha_1 - \alpha_0) + \ln\left|\frac{1-\alpha_1}{1-\alpha_0}\right| = 0$$

Both condition equations are solved commonly by an iteration procedure, yielding the best fitting parameters α_0 and α_1, so that k_p, r and x_{stat} are determined.

This kind of fitting is sensitive to correctly extracted experimental data and the reasonable correspondence of measured and calculated mass and rate values is convincing. The determined layer thickness values are small enough to meet the assumption, that film flow-down has not to be taken into account. Application of the described evaluation scheme to TG tests with porous B_4C is not allowed. The additional B_2O_3, consumed for pore filling, does not contribute to barrier layer growth but is registered in the mass effect, so that layer thickness growth would be overestimated.

A-5. Tentative parameters values for application

A-5.1 Parabolic B_2O_3 barrier layer growth coefficient k_p

Assuming independence of the oxidation rate coefficient on the composition of the atmosphere and an Arrhenius term for the temperature dependence defines the function type:

$$k_p = k_p^0 \exp\left(\frac{-Q_p}{RT}\right)$$

The results of the evaluation of TG experiments on dense B_4C pellets performed at 800 and 1000 °C have been used for fitting. The actual recommendation (for any condition except steam starvation) is the following correlation:

$$k_p = 3.476 \cdot 10^{-3} \exp\left(\frac{-118150}{RT}\right)$$, Q_p in J/mol K, k_p in cm^2/min

A-5.2 Evaporation of boron oxide B_2O_3

The direct evaporation of B_2O_3 and that of boric acids shall be assumed as additive, i.e. $r = r_{ox}+r_{ac}$ (indices ox for oxide and ac for acid). The temperature dependence of B_2O_3 evaporation and an upper limit for its rate are determined on basis of the kinetic theory of gases: In thermal equilibrium and for any gaseous molecule the evaporating mass per surface area and time is given by [6]:

$$r_{ox,\max} = \frac{m}{At} = \frac{0.4p}{\sqrt{RT}}$$, m=mass, A=area, p=partial pressure

This is the theoretical limit for the evaporation rate, since most of the evaporating molecules will re-condense in thermal equilibrium and only a part of them may escape. The calculated partial pressure of B_2O_3 for oxidising conditions [7], confirming [8], is inserted into the above given equation. A good fit to an Arrhenius dependence is obtained, since the square root factor cannot distort the strong temperature dependence of the pressure. The resulting equation for the evaluated upper limit of the B_2O_3 evaporation rate is:

$$r_{ox,\max} = 3.0 \cdot 10^{11} \exp\left(\frac{-382900}{RT}\right)$$, r in g/cm^2 min, Q in J/mol K

The temperature dependence can be taken as derived above, but a pre-exponential fraction factor is to be included for reduction to realistic evaporation rates. This factor, determined by the flow conditions in the different experimental programs (TG, BOX, VERDI), is expected to be independent of gas composition and only “gas” flow rate dependent. Assuming no information from this side and as preliminary choice for actual estimations a constant factor of 0.01 is introduced, which compares reasonably to the TG results and to experiments on evaporation into vacuum [9]. The strong temperature dependence is responsible for the insensitive influence of this factor on the horizontal position of the Arrhenius line, but improvement is needed in this point.

So the following estimation, satisfactorily defined only in the activation energy, is obtained and proposed for preliminary application:

$$r_{ox} = 3 \cdot 10^9 \exp\left(\frac{-382900}{RT}\right)$$, r_{ox} in g/cm^2 min, Q in J/mol K

The extremely strong temperature dependence, far above the treatment in actual modelling, predicts much higher reaction rates for extremely high temperatures than previously expected.

A-5.3 Evaporation of boric acids

Strong enhancement of evaporation was determined in the TG experiments in "wet" atmosphere compared to "dry" conditions. If no complete surface coverage by boric acid must be assumed, introduction of an additive evaporation term is reasonable. Accordingly, a different temperature dependence can be easily taken into account. Boric acids evaporation should be restricted to their stability range and literature results might be available for a more basic evaluation, which even might distinguish the transfer for both types of acid.

Instead, the following evaluation is based on the TG results in order to get an estimated formulation. The directly measured evaporation rates in the low temperature range are even much faster than the above given theoretical limit for B_2O_3, so that they are only due to boric acid. Their temperature dependence is found to be much lower. In contrast, the dependence on the humidity supply or content and the dependence on the gas flow rate have been found to be strong, practically linear. All results are taken into account by the following function:

$$r_{ac} = f_{ac} \cdot j_{gas}^{TG} \cdot \frac{p_{H2O}}{p_{tot}} \exp\left(\frac{-Q_{ac}}{RT}\right)$$

Fitting to the evaporation in wet argon (10 ltrs./h Ar for system purging plus 10 ltrs./h Ar, saturated with steam at 60 and 20 °C, p_{H2O}/p_{tot}= 0.2031/2 and 0.0238/2, respectively, flow cross section diameter 30 mm, and j_{gas}(TG)=0.0841 g/cm^2 min) resulted in Q_{ac}=61340 J/mol K and f_{ac}* j_{gas}(TG) = 0.3814 g/cm^2 min, so that one obtains (Fig. A3):

$$r_{ac} = 4.535 \cdot j_{gas} \cdot \frac{p_{H2O}}{p_{tot}} \exp\left(\frac{-61340}{RT}\right)$$, r_{ac} in g/cm^2 min, Q in J/mol K

In comparison with the TG series on the evaporation in argon it can be concluded that those experiments did not provide absolutely dry conditions, but saturation temperatures far below 0 °C. All other TG results on evaporation are in good agreement with the given correlation. Application for other experimental programs is possible simply by inserting the corresponding factors j_{gas} and p_{H2O}/p_{tot}.

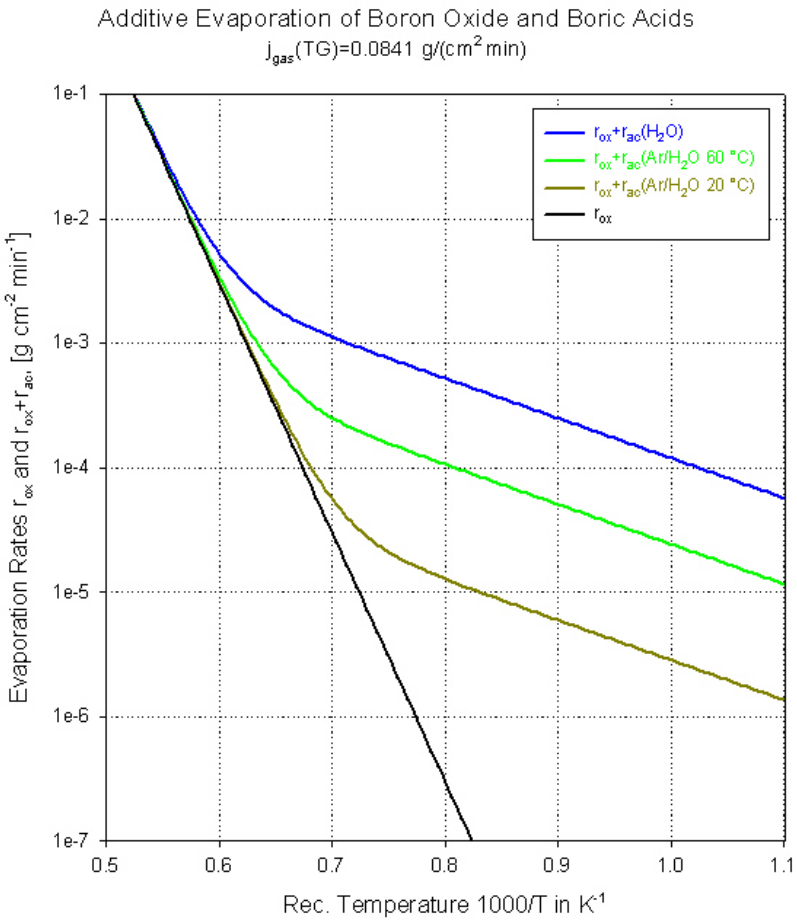

Fig. A3: Evaporation rates for boron oxide r_{ox}, boric acids r_{ac}, and their additive combination, resulting from assumed validity of the above given function for r_{ox}, and fitting r_{ac} to TG results for B_2O_3 evaporation in "wet" argon. (The combined evaporation curves illustrate the case j_{gas}(TG)=0.0841 g/cm² min.)

A-5.4 Stationary B_2O_3 layer thickness calculated from the actually proposed parameter values

According to the relation $x_{stat}= \rho_p k_p/r$ the stationary B_2O_3 layer thickness can be calculated and plotted in form of contour lines as function of the factor p_{H2O}/p_{tot} as one variable and temperature as the other. This plot is given in Fig. A4 more to show the trends than to claim absolutely correct values, as those depend strongly on the above given parameters, and especially their temperature dependence. The result, which seems to be realistic, will change in an application to other experimental programs, more in the values than in the trend.

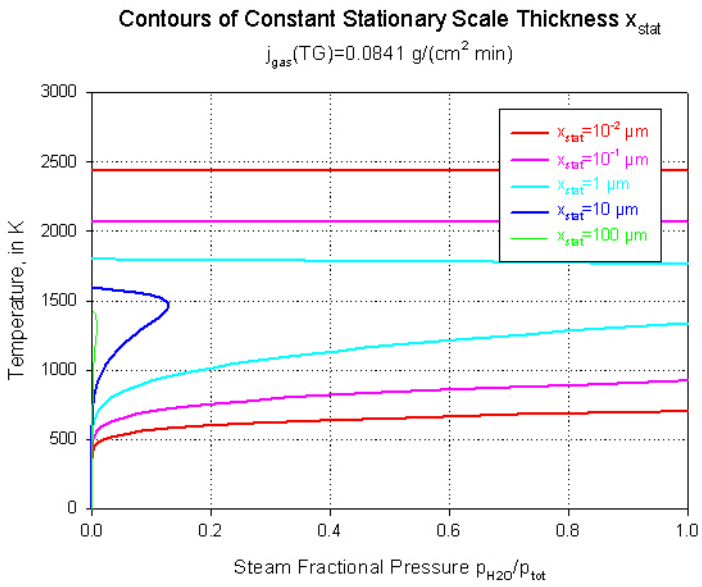

Fig. A4: Thickness contours of the B_2O_3 layer for stationary conditions as function of fractional steam pressure and temperature. (The case $j_{gas}(TG)=0.0841$ g/cm^2 min is illustrated.) For constant and not very high temperature the values tend to decrease from "dry" to "wet" conditions

A-5.5 B_4C oxidation according to actually proposed parameter values

According to Eqs. (9) and (15) the consumption of B_4C proceeds with the rate:

$$\frac{dy}{dt} = \frac{M_e}{2M_p}\frac{\rho_p}{\rho_e}\frac{k_p}{x} \quad (8), \text{or} \quad \frac{dy}{dt} = \frac{M_e}{2M_p}\frac{\rho_p}{\rho_e}\left(\frac{dx}{dt} + \frac{r}{\rho_p}\right) \quad (2), \qquad r=r_{ox}+r_{ac}$$

In short term the rate is determined by k_p and decreases with barrier layer growth (see Eq. 15), in the stationary long term (dx/dt=0) the rate is proportional to r (see Eq. 9). In between the layer thickness evolution determines the non-stationary general case, which is to be considered for temperature-transient applications.

A-6 Summarising comments on thermogravimetry results and evaluation

- Bare boron carbide (B_4C) reacts on the exposure to oxidising atmosphere by formation of a barrier layer of B_2O_3, which is liquid above ~ 450 °C. Violent mass gain during the transient heat-up phase of tests indicates this. Specimens with open porosity consume a part of the formed oxide for pore clogging in addition to scale growth during an initial phase of fast B_4C consumption.
- The time dependence of gross scale thickness growth is consistent with parabolic kinetics according to a strongly temperature dependent parabolic rate coefficient, which is the B_4C dependent parameter.

- Continuous fractional scale evaporation counteracts against scale growth, as it proceeds with a constant rate, determined by temperature, atmosphere composition and flow rate. For this parameter, determined by the thermal-hydraulic boundary conditions, two mechanisms are distinguished below.
- Interaction of both parameters results in non-stationary conditions, which have to be considered during the initial phase of the reaction and especially during temperature transients. Low temperatures require long periods for establishing stationary conditions due to small reaction and evaporation rates. At increasing temperatures stationary scale thickness tends to establish faster.
- In dry atmosphere, in the present context an unrealistic condition, studied for comparison, the downward flowing of the liquid cover layer has indeed been observed, as expected, so that the above described behaviour cannot develop further. This is explained by the limited scale evaporation in dry atmosphere, resulting in a higher stationary thickness. In wet atmosphere such an effect was not observed in any test. This is explained by the stability of a thin liquid film under conditions of fast dynamical equilibrium of formation and evaporation.
- The faster evaporation in wet atmosphere is due to formation of boric acids (ortho and meta forms in principle) in contact with water molecules and their transport with the steam flow. In view of the fast transfer of boric acid it is plausible to assume no complete coverage of the boron oxide by boric acid.
- It follows that direct boron oxide evaporation and indirect transport via boric acid can be treated as additive mechanisms. The limited thermal stability of boric acids should limit the regime of the latter mechanism. The observed temperature dependence of the total evaporation seems to support an independent treatment with different temperature and flow rate or composition dependencies.
- In the two temperature regimes distinguished by mainly boron oxide or boric acid evaporation, respectively, the stationary scale thickness should show reverse temperature dependence trends: Decrease with increasing temperature (HT range) and decrease with decreasing temperature (LT range). Due to the strong temperature dependence of B_2O_3 evaporation very high reaction rates are predicted for extremely high temperatures.
- Facing the described complications a final description has not yet been reached. In the considered context it will be most important to find consensus for the HT range, the uncertainties concerning the lower temperature range are less important. Moreover, the assumption of boron carbide exposure to steam is not valid until the control rod gets perforated. Consequently, the kinetics of B_4C oxidation together with its exposure to the atmosphere have to be treated in a coupled and reasonably simplified way.

Appendix B:

Literature results and mechanistic questions

Review articles [10, 11], containing information on B_2O_3 and B_4C, report melting of crystalline B_2O_3 at 723 K and its glassy structure above. Calculated B_2O_3 partial pressure and evaporation rate data in temperature dependence [7] and measured evaporation rates into vacuum (1000 to 1200 °C) [9], the latter determined in a B_4C oxidation study (O_2, 600 to 1200 °C), are mentioned. Formation of boric acids (HBO_2 and H_3BO_3) and enhanced evaporation in water vapour containing atmosphere is reported in a study on B_2O_3 melts [12]. B_2O_3 barrier layer formation and volatility is known to influence the oxidation of other materials as B_4C-SiC [13] and ZrB_2-SiC composites [14] in competition with formation of more stable boro-silica glass layers.

Many details of the oxidation of B_4C, especially referring to initial phases, are not clear. Influences might be due to adsorbed humidity and surface impurities, preferential oxidation of carbon or boron and enrichment of the other component at the surface [9], wetting conditions for B_2O_3 condensation, capillary effects in the filling of open porosity, escape of gas from the partially covered surface, limitation of the resulting B_4C reaction rate due to bulk atmosphere/surface transport kinetics or formation of a closed barrier layer of B_2O_3, which is considered above.

Acknowledgements

The experimental work described in this report was co-financed by the European Commission under the EURATOM 5th Framework Programme on Nuclear Fission Safety 1998-2002.

References

1 B. Adroguer et al.,
Core loss during a severe accident;
Proc. FISA-2001 EU research in reactor safety, Luxembourg,
12 - 14 Nov. 2001, p 350

2 B. Adroguer et al.,
Core loss during a severe accident;
Nucl. Eng. Design 221, (2003), 55 - 76

3 M: Steinbrück, A. Meier, U. Stegmaier, L. Steinbock, J. Stuckert,
Box tests on the oxidation of B_4C at high temperatures; Test data report,
SAM-COLOSS-P026, May 2002

4 M: Steinbrück, W. Krauss, G. Schanz, H. Steiner, A. V. Berdyshev,
M. Veshchunov,
FZK separate-effect tests on B_4C oxidation; Final analysis report,
SAM-COLOSS-P054, Feb. 2003

5 P. Kofstad,
High-temperature oxidation of metals; Wiley, (1966), 234-235

6 R. W. Pohl,
Einführung in die Physik; Band 1, Springer, (1959)

7 R. H. Lamoreaux, D. H. Hildenbrand, L. Brewer,
J. Phys. Chem. Ref. Data Vol. 16, (1987), 419-443

8 Y. S. Touloukian,
Thermophysical properties of high temperature solid materials; Vol. 4, Pt. 1,
(1967), 89-90

9 V. A. Lavrenko, A. P. Pomytkin, P.S. Kislyj, B. L. Grabchuk,
Oxidation of Metals; Vol. 10 No. 2, (1976), 85-95

10 G. Heller,
Boron Compounds; Gmelin Handbook of Inorganic Chemistry, 3rd Supplement Vol. 2, Springer (1987)

11 G. Heller,
Boron Compounds; Gmelin Handbook of Inorganic Chemistry, 4th Supplement Vol. 2, Springer, (1993)

12 J. T. Wenzel, D. M. Sanders,
Phys. Chem. Glasses, Vol. 23, (1982), 47-52

13 R. Telle,
Oxidation behavior of B_4C-SiC composites with various microstructures; Boron-rich Solids, Albuquerque, (NM), 1990, American Institute of Physics, Conference Proceedings No. 231, (1991), 553-560

14 H. C. Graham, H. H. Davis, I. A. Kvernes, W. C. Tripp,
Microstructural features of oxide scales formed on zirconium diboride materials; Ceramics in Severe Environments. Materials Science Research Vol. 5, Plenum Press, (1971), 35-48